GEEA
Research article
Geochemistry: Exploration, Environment, Analysis
Published online August 16, 2019
https://doi.org/10.1144/geochem2019-009 | Vol. 20 | 2020 | pp. 129–154

Application of ultrafine fraction soil extraction and analysis for mineral exploration

R. R. P. Noble[1]*, P. A. Morris[2], R. R. Anand[1], I. C. Lau[1] & G. T. Pinchand[1]

[1] CSIRO Mineral Resources, 26 Dick Perry Avenue, Kensington, WA 6151, Australia
[2] Geological Survey of Western Australia, 100 Plain Street, East Perth, WA 6004, Australia
RRPN, 0000-0001-5827-1020; ICL, 0000-0002-5026-3189
* Correspondence: ryan.noble@csiro.au

Abstract: The need to innovate to advance exploration success is ongoing and, while regional geochemical surveys are common, increasing the data we collect and improving survey results has stagnated. A new adaption of existing methods known as UltraFine+™ extracts the <2 μm fraction of soils and sediments, which is then analysed and combined with spectral mineralogy proxies and physicochemical properties to improve targeting for Au and base-metal exploration. We applied the UltraFine+™ workflow to three small orientation site studies in Western Australia, and reprocessed archived regional soil samples from the Geological Survey of Western Australia to test the method. The orientation programme (*c.* 200 samples) involved samples from the Leonora and Sir Samuel 1:250 000 map sheets, an area that hosts known major Au and base-metal deposits. We then applied this approach to the Kingston 1:250 000 map sheet area, analysing a further 300 samples in a region on the Yilgarn Craton margins that is essentially greenfields, as there has been little exploration and the original geochemical survey data were heavily censored due to the abundance of transported regolith dominated by quartz-rich sand. The archived samples were specifically selected soils (sheetwash or sandplain) with a component of Quaternary–Tertiary transported cover. Results at the orientation test sites (Telfer West, Tooting Bec and DeGrussa) were promising. Importantly, the study revealed a marked decrease in censored results for Au (from 63% to 10% below detection limit). Geochemistry and some example indices for mineral exploration and lithology mapping, as well as example maps using the additional spectral mineralogy proxies or particle-size variation, are presented. The application of the <2 μm particle-size separation and the UltraFine+™ workflow importantly demonstrate the additional value from (re-)assaying regional soil and sediment samples to generate new targets and improve regional geochemical maps. This is an exercise that can be applied to new greenfields surveys and, when exploration budgets are lean, to archived samples.

Keywords: covered terrains; spectral mineralogy; regolith; UltraFine+™; particle size; clay

Received 14 February 2019; **revised** 24 June 2019; **accepted** 25 June 2019

Traditional, near-surface geochemical techniques have been reasonably effective in mineral discovery but to explore in deeper transported cover and find new resources, as demanded by a growing global population, innovative methods are required. Recently, a new adaption of methods to extract the ultrafine fraction of soils and sediments, assay the geochemistry, and combine this with additional spectral and physicochemical properties (Noble *et al.* 2019) has shown some major benefits for Au and Cu exploration. This UltraFine+™ workflow uses less sample, provides more data and reduces the nugget effect for Au with solid reproducibility. Also, few samples are below detection limits for Au (0.5 ppb), even in dune sands, for example, because the technique avoids dilution from the bulk Si-rich matrix, concentrating clays and iron oxides that host most elements of exploration interest like Au. However, despite these potential benefits, the new workflow has not been applied to exploration examples such as orientation studies or regional geochemical surveys.

Regional geochemical surveys are conducted routinely with sample densities from one per km^2 to one per 100 km^2 (Salminen 2011) by government organizations, companies and individuals in all parts of the world. Many of these surveys use traditional methods which aids comparison, particularly across state and country borders or with other datasets (Smith *et al.* 2009; Reimann & de Caritat 2012; Li *et al.* 2014).

The resulting surveys and data are instrumental in providing context and background for a range of applications, environmental baseline, remediation, agriculture, forestry and mineral exploration. These surveys are common first-pass approaches in mineral exploration when exploring for bedrock-hosted mineralization (Morris 2013). However, to improve the application for mineral exploration in particular, especially with respect to cover, these results may not provide the best information for trace and pathfinder elements.

Regarding mobilization of trace metals through cover, results show these transported elements will be small, seasonally-variable (Anand *et al.* 2014, 2016*a*) and commonly positively charged. These charged metals and metalloids will ultimately be adsorbed onto the surfaces of clay minerals, organic complexes and Fe oxides which are common in cover sediments and have the ability to exchange these charged cations (Hawkes & Webb 1962; Hall 1998). Separating these small fractions (*c.* <2 μm) to improve results has been shown to be valuable (van Geffen *et al.* 2012; Noble *et al.* 2013, 2019; Carlson 2016; McClenaghan & Paulen 2018; Sader *et al.* 2018).

By adjusting methods for regional surveys, significant improvements can be made for mineral exploration. The Au data for a regional stream sediment survey in Canada were deemed useless as the nugget effect was too extreme and reproducibility almost non-existent in the bulk sediments. However, refining the sample particle size to <4 μm demonstrated a greatly improved reproducibility on a select few samples that could be scaled up to the survey (Arne & MacFarlane 2014). Baker *et al.* (2015) re-assayed historical samples to successfully demonstrate the value of using newer technology and improved analytical sensitivity. In this case, they

clearly identified a known major deposit that was missed in earlier regional geochemical surveys and generated new targets (Baker *et al.* 2015).

The nugget effect is well known in mineral exploration and processing. The nugget effect means that however well mixed samples are, there will be significant variations in value. This variability is most problematic where there are small-scale structures such as narrow veining or coarse Au particles resulting in biased estimations for exploration potential or resource definition (Harris 1982; Nichol *et al.* 1989; Wang *et al.* 1995; Dominy *et al.* 2001). While statistical approaches were used to quantify this effect (e.g. Stanley 2006), there is a lot of potential to adjust the physical sample particle size down to exclude 'nuggets' to be analysed and for increased reproducibility.

Detection limits have often been problematic in regional surveys, with Au values below detection resulting in highly skewed data and creating problems for statistical analysis (Leybourne & Rice 2013). For example, the Mount Phillips survey comprised 89% censored data of samples that were below detection for Au (Sanders *et al.* 1997). The results from decades previously are much more problematic, with numerous key elements not analysed or detection limits that were so high the majority of data are censored and those that are reported are just around the detection limits, all of which can cause interpretation issues. A common practice to deal with data below detection for statistical evaluation is to replace censored data with a value equal to half the lowest detection limit (Grunsky 2010; Reimann *et al.* 2010) or to impute values below detection based on a statistical model. However, the preferred option is to have data with a detection limit low enough to allow for the definition of background levels.

Other regional surveys of the past have suffered from censored data, such as the Geological Survey of Western Australia's (GSWA's) Kingston 1:250 000 map sheet that was sampled, analysed and reported by Pye *et al.* (2000). The Kingston map extends NE of the Yilgarn Craton and into the Earaheedy Basin. The region is underexplored based on tenement uptake (Fig. 1) compared to the Sir Samuel (Kojan *et al.* 1996) and Leonora (Bradley *et al.* 1995) map sheets SW of the Earaheedy Basin. Here, there are more samples with detectable Au, some outcrop and residual regolith, and numerous large and well-known Au deposits in the area to maintain exploration interest. Figure 1 shows the location of these key regions that are part of the broader regional analysis conducted in this study. Figure 2 shows the map sheets discussed, surrounding areas, major deposits and the samples that are potentially available for further analyses.

The large number of samples in Figure 2 all have multi-element geochemistry associated with them but minimal additional data, excluding regolith and geological description. While these are of utmost importance, adding spectral mineralogy, colour and other parameters to geochemistry is valuable but is not commonly done, and certainly not integrated. Industry and research groups are looking to develop big/more data and how best to use them. The integration of spectral data and other physicochemical parameters is perceived as the next generation of routinely collected soils data (Winterburn *et al.* 2019).

Examples of regional geochemistry and the addition of spectral mineral proxies have been tested (Reeves & Smith 2009), and resulting maps combined with geochemistry have been shown to have value in agriculture. The use of reflectance spectroscopy in digital soil mapping (pedometrics) has increased greatly in recent years, with soil C, pH, CEC, Eh and moisture predicted using partial least-squares regression (PLSR) from spectral measurements on soils (for a recent review see Fang *et al.* 2018). This same approach has not been applied to mineral exploration and is eminently achievable. Spectral data were collected in this study, yet have been a lesser component of the evaluation, and that integration is not the focus of this research.

Noble *et al.* (2019) demonstrate an innovative shift in method development and analytical considerations using fine soil fractions. In this paper, we apply the new UltraFine+™ method to a number of exploration sites and, importantly, demonstrate the additional value to be gleaned from (re-)assaying regional soil samples with newer and improved methods to generate new targets and regional geochemical maps.

Geological settings

Sir Samuel/Leonora region

The Sir Samuel map sheet lies between latitudes 27°00′ S and 28°00′ S, and longitudes 120°00′ E and 121°30′ E, and includes major Au mining regions such as Agnew, Bronzewing and Darlot,

Fig. 1. (**a**) Location showing the major map sheet areas, as well as the approximate location of orientation sites used in this study. (**b**) The map sheets with green shading representing current active tenements (tenement map is from GeoView, GSWA accessed 12 September 2018).

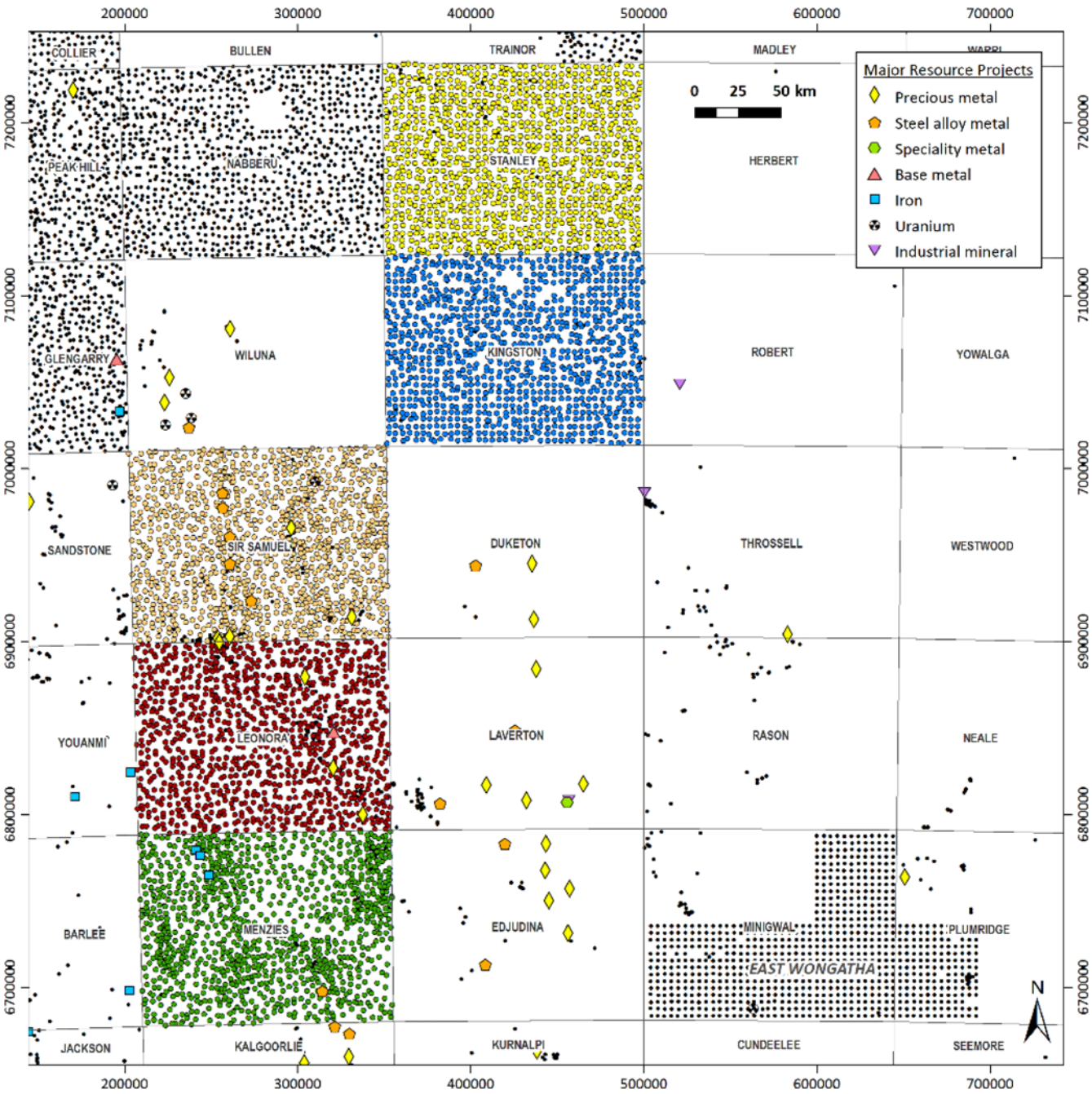

Fig. 2. Regional geochemical samples from the GSWA database related to this current project and potential analysis using the UltraFine+™ method. Major resource projects are mapped; note there is none in the Kingston map sheet.

with significant Ni endowment at Leinster and Mount Keith among others. The map sheet takes its name from the abandoned mining town of Sir Samuel (Kojan *et al.* 1996) (Figs 1 and 2). The Leonora map sheet located immediately south of the Sir Samuel map sheet lies between latitudes 28°00′ S and 29°00′ S, and longitudes 120°00′ E and 121°30′ E, and includes the major Au mines of Sons of Gwalia (Leonora), Emu (Lawlers) and Tarmoola–King of the Hills (Bradley *et al.* 1995) (Fig. 2). The sheet is named after the biggest population centre in the region – the township of Leonora.

The geology of this area is typical of the northern Yilgarn Craton, and comprises variably distributed Archean-aged (2.6 Ga) granites and granitic gneiss with extensive NE-trending, elongate greenstone belts (Williams 1975; Myers 1997). The dominantly mafic and ultramafic volcanic greenstones occur in a series of belts including the well-endowed Norseman–Wiluna belt, along with the Yandal and Dingo Range belts (Myers & Hocking 1998; Morris & Sanders 2001). The elevation ranges from 437 to 612 m asl (above sea level) (Bradley *et al.* 1995) The topography is gently undulating, with upland areas that have extensive ferruginization or silcrete armouring that led to erosional breakaways and stony plains, with much of the lower, broad depositional plains composed of colluvial/alluvial sheetwash plains, sandplains and drainage channels.

The soils are dominated by kaolinite and quartz with small amounts of goethite, hematite and muscovite, and they show weak structure and little development of distinct A and B horizons (Anand & Paine 2002). The annual rainfall is highly variable and *c.* 200–210 mm. Rain falls more frequently in the first half of the year and is tied to northern cyclonic activity (Bradley *et al.* 1995; Anand & Paine 2002). The flora is dominated by mulga (*Acacia* sp.) shrublands with spinifex (*Triodia* sp.) on sandplains, and *Eucalypt* sp. in the ephemeral drainages. In the broad saline drainage channels, halophilic saltbush, bluebush and samphire species are present.

Kingston region

The Kingston map sheet lies between latitudes 26°00′ S and 27°00′ S, and longitudes 121°30′ E and 123°00′ E, and includes no major mining regions compared to the other regional sites used. Mount Eureka on the western edge of the greenstone belt of the same name produced 20 kg of Au in the early 1930s as the only record of sizeable metal extraction (Pye *et al.* 2000) (Figs 1 and 2).

The geology of this area includes the NE Yilgarn Craton with Archean-aged (2.6 Ga) granites and granitic gneiss and greenstone belts (Williams 1975; Myers 1997). This is overlain by a 5 km-thick package of sedimentary rocks of the Proterozoic 1.6–1.8 Ga comprising the Earaheedy Basin. Other dolerite and Patterson Formation rocks are present to the north, but do not cover the area studied here. The Frere Formation covers the mapped basin sediments in the southern section of the Kingston map sheet, and this unit consists of shales interbedded with iron formation and chert, and uncommon lenses of limestone (Pye *et al.* 2000).

The elevation ranges from 440 to 600 m asl. The topography is gently undulating, and is broadly classified into four regions by Pye *et al.* (2000): (1) upland areas corresponding to resistant Archean greenstone, Proterozoic rocks and Permian rocks; (2) areas of sandplain and aeolian material developed over Archean–Permian rocks, particularly in the SW; (3) broad sheetwash plains and valleys; and (4) areas proximal to, and including, salt lakes.

The soils are commonly poorly developed, with little pedogenesis, and rarely show development of distinct A and B horizons. Soils are siliceous, and quartz grains are commonly coated with clay-rich or iron-rich material (Pye *et al.* 2000) showing a reddish brown colour. The annual rainfall is highly variable and *c.* 200–250 mm. Rain falls more frequently in the first half of the year and is tied to northern cyclonic activity, although winter depressions may also provide precipitation to the region (Pye *et al.* 2000; Anand & Paine 2002). The flora is dominated by mulga (*Acacia* sp.) shrublands with spinifex (*Triodia* sp.) on sandplains, and Mallee *Eucalypt* sp. in other areas. The southern third of the map sheet and many of the samples used in this study are on a sandplain regolith setting. Similar to the Sir Samuel area, halophilic saltbush, bluebush and samphire species are present in the broad saline drainage channels.

Telfer West

The Telfer West prospect is located 25 km NW of Newcrest's major Au–Cu mine at Telfer (Fig. 1). The potential mineralization zone is under 50–80 m of transported cover. The cover is commonly Quaternary–Tertiary dune sands and underlying this are Permian glacial sediments that are highly weathered. Underneath the cover is very low-grade supergene Au in the weathered oxide zone of the Proterozoic saprolite. Recent and historical drilling indicates that the area contains several zones of high-grade Au mineralization within a substantial volume of stockwork veining. Geochemistry of the Proterozoic rocks indicates elevated As, Bi and Co as potential pathfinder elements. Exploration at Telfer West is targeting Au mineralization in a similar stratigraphy to the host units at Telfer. A dome structure has a core of Isdell Formation overlain by the Malu Formation, Telfer Formation and sediments of the Puntapunta Formation. These units are the main hosts of Au–Cu mineralization at Telfer (Encounter Resources 2016). The vegetation comprises sparse shrub-steppe with the dominant *Triodia basedowii* ('hard spinifex') and *Eucalyptus* sp. communities, and grasslands on alluvial channel sediments (Kendrick 2001). The broad depositional alluvial/colluvial/aeolian plains have a mix of *A. ancistrocarpa* and *Triodia* sp. The climate is semi-arid with average maximum and minimum temperatures of 34.1 and 19.4°C, respectively. The annual rainfall averages 367 mm, with most rain in the summer (Telfer weather station: Bureau of Meteorology 2013).

Tooting Bec

The Tooting Bec prospect is located 2 km SW of the Cannon Au mine and *c.* 30 km east of Kalgoorlie (Fig. 1) in the Yilgarn Craton, and is part of a major Archean-age greenstone belt of *c.* 2.7 Ga. The region is typical of the orogenic Kalgoorlie Au deposits, with the target mineralization in strongly sheared, mafic and ultramafic rocks. These rocks strike northeasterly and dip to the west. The mineralization is associated with biotite, calcite, chlorite, albite and pyrite alteration. High-MgO basalts, komatiites and related intrusives underlie the area. Black shale horizons, monzogranite and diorite dykes are present. The prospect is covered by shallow calcareous and/or ferruginous soil. The *in situ* regolith profile is shallow and it is commonly less than 20 m thick over the saprock. Calcrete nodules are common in the upper pats of the profile. The area is semi-arid with average maximum and minimum temperatures of 25.3 and 11.7°C, respectively. The rainfall averages 267 mm annually (Kalgoorlie–Boulder airport weather station: Bureau of Meteorology 2018). The area consists of eucalypt-dominated open woodland with an understorey of shrubs and grass.

DeGrussa

DeGrussa is located in the Proterozoic (*c.* 2 Ga) Bryah Basin that lies adjacent to the Archaean Yilgarn Craton to the south and the Archean granite Marymia Inlier to the north, and is part of the Capricorn Orogen (Fig. 1) (Noble *et al.* 2017). The geology has been discussed more by Adamides (1998) and Hawke *et al.* (2015). The dominant underlying lithology is sedimentary and volcanic rocks with argillaceous sandstones and conglomerates (Hawke *et al.* 2015). The elevation of the area is generally between 560 and 570 m asl. The deposit comprises high-grade Cu–Au in sulphide assemblages and also has a sizeable supergene Cu–Au oxide resource. DeGrussa is located on the edge of a palaeochannel in a colluvial/alluvial plain (González-Álvarez *et al.* 2015). The relatively flat surface hides a more complex regolith and the overlying transported units vary in thickness from a few metres directly over DeGrussa, to *c.* 30 m. The palaeochannel is up to 100 m in thickness. Residual uplands occur to the east and south of the deposit. Soils are dominantly acidic, sandy with red-brown silicified hardpans and a lack of significant calcrete horizons except in palaeochannels. Prominent soil minerals include quartz, kaolinite and Fe oxides. The regolith in this region is similar to that of the northern Yilgarn, as seen in the Sir Samuel/Leonora region, with the DeGrussa region receiving more rainfall, *c.* 240 mm of rain annually. Vegetation is *Acacia-aneura*-dominated shrubland with some seasonal grasses, especially in the alluvial channels.

Methods

Soil and regolith samples

For the large regional maps, more than 500 soil samples were sought from the stored historical materials at GSWA's core storage facility in Carlisle, Western Australia. Using the GSWA GeoView spatial data, we isolated a total of 200 soil samples that were located around major mineral deposits in the Agnew, Leonora and Yandal greenstone belt regions (Fig. 3). We then determined another 300 samples in the Kingston map sheet over the Earaheedy Basin, and covered *c.* 50% of that 1:250 000 map sheet as a 'greenfields' test case. Figure 2 shows the number of available samples in the areas considered for this study, with Figure 4 showing the final selected samples and the only mineralization known in the area.

Regional orientation samples crossed two major fieldwork programmes by GSWA – the Leonora and Sir Samuel 1:250 000 map sheets that are summarized in reports by Bradley *et al.* (1995) and Kojan *et al.* (1996), respectively. Samples were filtered according

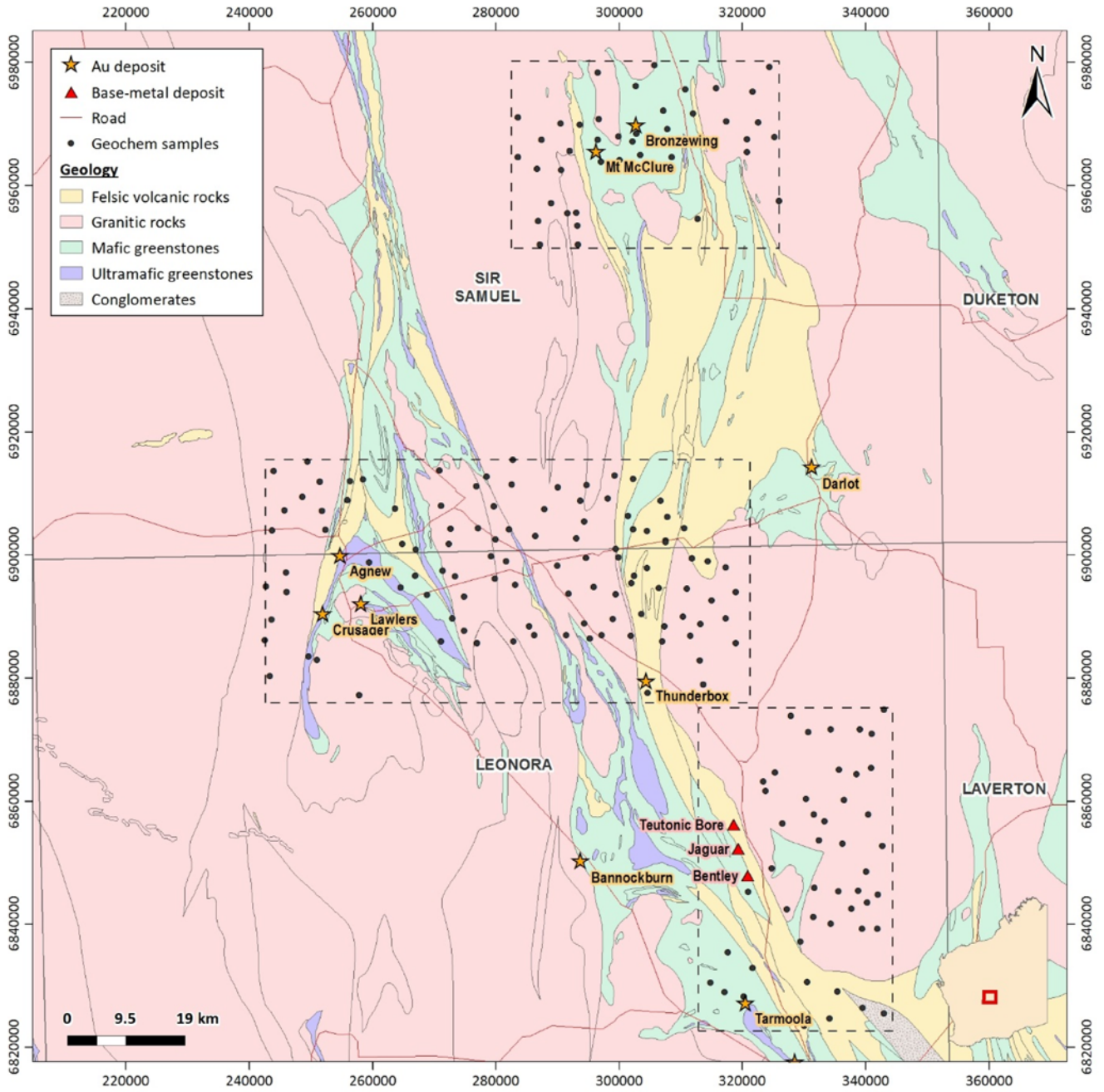

Fig. 3. Selected samples for the orientation test case, filtered by sample type and proximity to some prominent Au and base-metal deposits and areas of interest (dashed boxes). Inset box shows the same area but with all the smaller mineralization areas clearly depicting this as a resource-rich area (data from GSWA 2014).

to their proximity to three well-endowed Au areas (Agnew, Sons of Gwalia and Bronzewing) and then selecting only samples that were clearly not residual regolith/outcrop or stream drainages. Many of these samples were labelled as sandplain, sheetwash plain or soil. The stream sediment analysis in the Leonora and Sir Samuel regions revealed some Au and base-metal anomalies near the deposits, and we did not want to duplicate this obvious result but, rather, test the new method where previously results were ineffective when mapped in the original reports (Bradley *et al.* 1995; Kojan *et al.* 1996). Figure 3 depicts the location of the orientation samples. The Kingston map showed few detectable Au samples and no major Au resources; however, for consistency, the samples were filtered according to the same criteria as the other orientation surveys to remove vastly different sample types (outcrop regolith or stream sediments).

Once the ID of the samples required was ascertained, these were subsampled (*c.* 300 g) from the original 3–5 kg sample bags. Of the 200 samples collected as part of the orientation map, less than five looked to be unusual samples and may be indicative of proximal colluvium or possibly stream drainages. These were dominantly gravels and were noted during collection. All soil samples were screened to <2 mm for the UltraFine+™ analysis.

Other soils and regolith profile materials were collected from a number of orientation sites as part of the M462 project. These sites varied in sample number, target mineralization and knowledge of the underlying mineralization (Table 1). Locations are noted in the geological settings and Figure 1. These soils were submitted to a commercial laboratory for analysis using the UltraFine+™ method. The method is fully documented in Noble *et al.* (2019). In brief, the method uses less than *c.* 40 g of soil from the bulk (<2 mm) material. Gravity settling following dispersion of clays is used to separate the <2 µm size fraction. The term 'clay' herein refers to the <2 µm size particles (United States Department of Agriculture

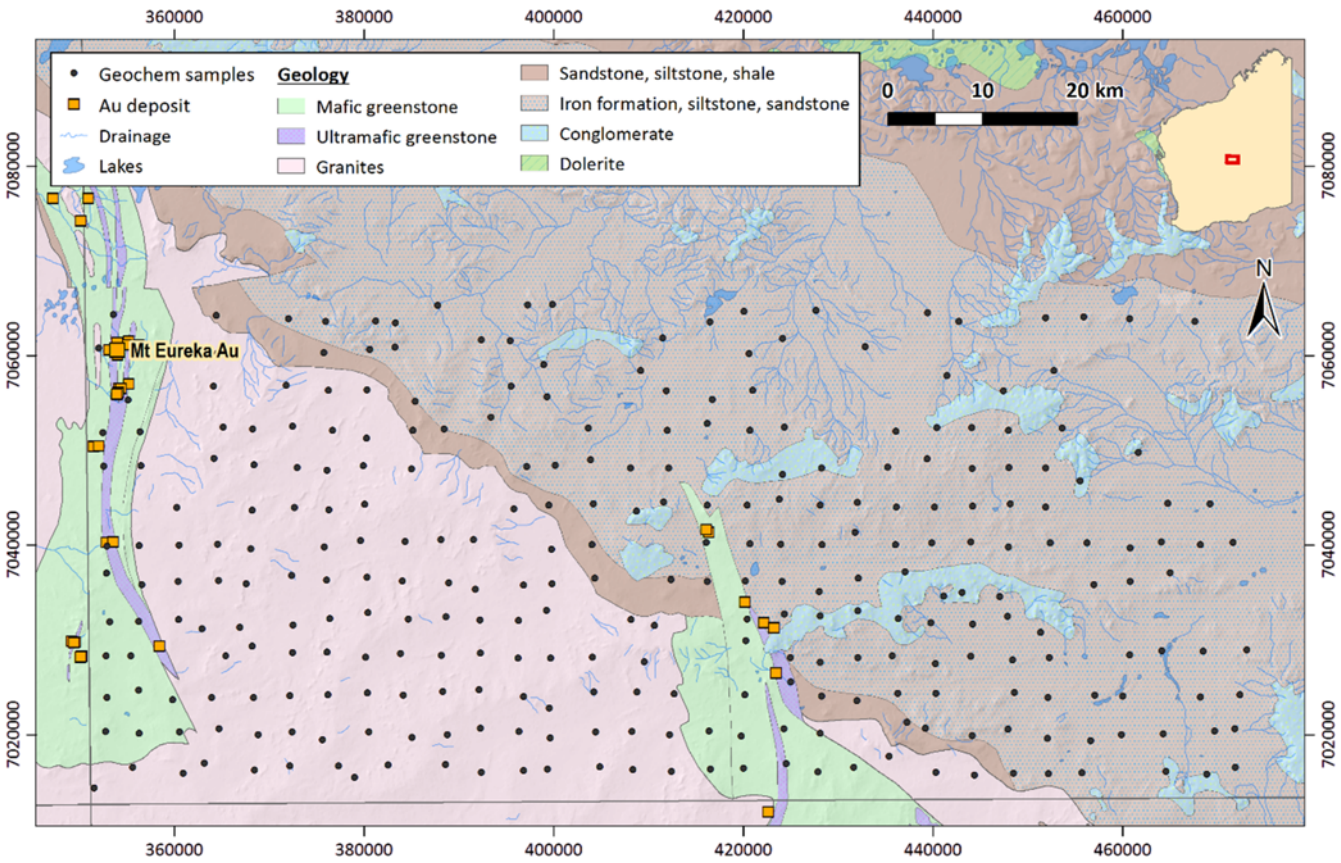

Fig. 4. Selected samples for the greenfield regional map covering the Kingston map sheet. The only mined Au deposit is labelled with other small, known Au mineralizations in the region.

classification: Gee & Bauder 1986). The separated fine soil fraction is analysed for a number of physicochemical properties such as pH, EC, particle-size distribution and spectral reflectance mineralogy, and then subjected to a microwave aqua regia digestion and analysis of the solution for *c.* 40 elements using inductively coupled plasma optical emission spectrometry (ICP-OES) and inductively coupled plasma mass spectrometry (ICP-MS).

Laboratory analysis

The standard UltraFine+™ extraction was MAR-04 (microwave-assisted aqua regia) offered through LabWest Pty Ltd, Perth, Australia. All partial extractions of the soils were analysed for a multi-element suite of *c.* 40 elements using ICP-OES (Perkin Elmer Optima 7300DV) and ICP-MS (Perkin Elmer Nexion 300Q). The microwave-assisted aqua regia digestion (LabWest MAR04) uses 0.2 g of soil subjected to an aqua regia digestion with a 100% mixture of 3:1 concentrated HCl:HNO_3. This is heated in a closed Teflon tube in a microwave (Anton Paar Multiwave PRO Microwave Reaction System).

Visible–near-infrared reflectance measurements were acquired on the bulk and separated samples using a Panalytical ASD FieldSpec4 standard-resolution spectroradiometer. The ASD FieldSpec4 measures electromagnetic reflectance and collects in the 350–2500 nm wavelength region, with a resolution of 3 nm at 700 nm, and 10 nm at 1400 and 2100 nm. The spectral bandwidths of the FieldSpec4 are 1.4 nm at 350–1000 nm and 1.1 nm at 1001–2500 nm, which are resampled to 1 nm to provide 2151 bands. A calibrated piece of PTFE (Spectralon) was used as the reflectance standard and measured before each set of soil measurements by raising the white reference standard on a lab jack directly below the downwards-facing probe. The samples were measured in their plastic vials and 40 scans were averaged into a single measurement. Processing of spectra was done using The Spectral Geologist (TSG) software to extract the main features reported as part of the UltraFine+™ workflow.

Conductivity and pH measurements were made at LabWest using a TPS AQUA-CP/A waterproof conductivity/total dissolved solids (TDS)/salinity/pH/temperature meter of 1:5 w/w soil/water ratio slurries for all samples collected in this study.

Particle size was measured using a Malvern Mastersizer 3000 in suspension using the HydroMV unit and dry bulk using the Aero S attachments. Both techniques assumed non-spherical particles and kaolinite as the dominant mineral with a refractive index of 1.45 (this is not dissimilar to the value for quartz or Fe oxides which also are common minerals with 1.51 and 1.456, respectively). The specific surface area (SSA) reported is the total area of the particles divided by the total weight using the assumed density of kaolinite and non-porous particles (Malvern Instruments 2011).

Table 1. *Details for the various smaller orientation surveys conducted using the UltraFine+™ method*

Orientation site	Size	Target mineralization	Transported cover	Type of cover	Samples
DeGrussa	Large mine	Cu–Au	2–30 m	Transported over residuum. Quaternary–Tertiary	Two soil traverses
Telfer West	Prospect	Polymetallic what?	30–60 m		Two soil traverses
Tooting Bec	Prospect	Au	?		Four soil traverses

Table 2. *Summary statistics for the Sir Samuel and Leonora regional soils using the UltraFine+™ method*

	% Censored	Minimum	Maximum	Mean	Median	SD	95th percentile
Ag	0.0	0.02	0.14	0.04	0.04	0.01	0.05
Al	0.0	34 900	171 000	95 675	93 700	24 409	142 000
As	0.0	3.4	32.1	7.7	7.3	2.9	10.8
Au	8.8	0.50	17.6	2.36	1.80	2.11	5.46
Ba	0.0	31.2	250	67.0	62.0	27.0	110
Be	0.0	0.7	2.8	1.6	1.6	0.3	2.2
Bi	0.0	0.20	1.30	0.47	0.40	0.16	0.80
Ca	0.0	310	5320	1835	1920	905	3543
Cd	46.1	0.05	0.16	0.08	0.07	0.03	0.14
Ce	0.0	29.7	113	60.1	58.4	13.7	84.3
Co	0.0	4.70	92.0	12.8	10.2	8.78	26.6
Cr	0.0	74	501	130	119	50	213
Cs	0.0	1.6	6.9	4.9	4.8	0.76	6.1
Cu	0.0	11.5	77.1	42.4	42.9	12.7	62.7
Fe	0.0	30 100	92 800	58 037	57 400	9717	74 950
Ga	0.0	8.38	47.2	26.2	25.0	6.01	40.5
Ge	0.0	0.11	0.77	0.37	0.36	0.14	0.62
Hf	0.0	0.07	1.1	0.33	0.26	0.20	0.75
In	0.0	0.03	0.11	0.08	0.08	0.01	0.10
K	0.0	2300	9290	4586	4580	1124	6577
La	0.0	15.4	76.5	39.6	38.2	10.2	59.7
Li	0.0	12.3	52.0	27.9	26.9	6.52	39.9
Mg	0.0	687	4900	1733	1690	696	3100
Mn	0.0	138	1540	483	465	227	888
Mo	0.0	0.600	19.9	2.01	1.90	1.38	2.73
Nb	0.5	0.50	1.4	0.94	0.90	0.13	1.1
Ni	0.0	10	1020	41	31	74	76
Pb	0.0	13	42	19	19	3.4	25
Pt	13.5	1.0	5.0	2.1	2.1	0.9	4.0
Rb	0.0	23.7	102	65.0	63.7	11.0	81.9
S	0.0	140	637	282	247	107	532
Sb	0.0	0.30	1.6	0.45	0.40	0.12	0.60
Sc	0.0	6.0	38	20	19	5.0	28
Se	0.0	0.490	1.95	1.19	1.18	0.196	1.54
Sn	0.0	0.90	3.6	2.5	2.5	0.32	3.0
Sr	0.0	12.7	60.9	34.0	35.0	9.00	49.2
Th	0.0	5.87	49.0	15.2	14.2	4.85	28.2
Ti	0.0	343	1530	713	688	155	997
Tl	0.0	0.2	0.6	0.4	0.4	0.1	0.5
U	0.0	0.760	6.24	3.08	3.09	0.804	4.31
V	0.0	64	204	135	135	21	171
W	0.0	0.2	0.9	0.4	0.3	0.1	0.6
Y	0.0	5.53	47.7	24.2	24.5	8.18	38.1
Zn	0.0	31.8	242	76.0	74.8	26.0	106
Zr	0.0	3.0	27	12	10	6.1	23
EC	0.0	7.33	484	30.0	22.4	40.0	68.8
pH	0.0	3.76	6.40	5.16	5.16	0.53	6.00
<2 µm*	0.0	10	87	62	65	16	82
2–50 µm*	0.0	9.0	81	28	25	12	48
50–125 µm*	0.0	0.0	8.7	0.4	0.0	0.9	1.8
125–250 µm*	0.0	0.0	2.6	0.3	0.0	0.5	1.5
250–2000 µm*	0.0	0.0	50	9.5	5.0	11.3	31
> 2000 µm*	0.0	0.0	1.5	0.2	0.0	0.3	0.8
SSA* ($cm^2\ g^{-1}$)	0.0	1544	70 612	39 874	40 296	16 284	64 002
Kaolin abundance	0.0	0.125	0.327	0.250	0.244	0.035	0.311
Ferric oxide abundance	0.0	0.048	0.123	0.090	0.090	0.015	0.114
Hematite/goethite	0.0	896.33	910.26	901.00	900.37	3.000	906.71

Elemental concentrations are in ppm except for Au and Pt which are in ppb. EC in µS/cm. Spectral scalars are standard output, refer to Noble *et al.* (2019). $n = 193$. SSA, specific surface area.
*Particle size distribution is for comparison only and currently overestimates clay and silt percentages.

Quality control and data treatment

For GSWA's regolith geochemistry assessment of precision, a value of <20% RSD (relative standard difference) was considered acceptable if the values of the elements detected were at least three times greater than the detection limit (Morris & Verren 2001; Morris 2013). The certified reference soil (CRM) OREAS 250 was incorporated into all geochemistry analyses for this study to assess accuracy.

Gold ($n = 26$) reported 309 ± 15 ppb (1σ) compared to the OREAS 250 CRM indicative value of 303 ± 13 ppb (1σ) using aqua regia showing excellent accuracy (the fire assay CRM result is 309 ± 13 ppb). Copper reported 49.6 ± 2.9 ppb (1σ), Ag 0.32 ± 0.07 ppb (1σ) <10% and Zn 95.3 ± 8 ppb (1σ). These results compare favourably to the CRM values of Cu (44.7 ± 1.3 ppb), Ag (0.26 ± 0.04 ppb) and Zn (82 ± 4.3 ppb). Elements with high variance were Al, Cs, Ga, Ge, K, Sb and Ti. Not surprisingly, many of these are highly resistant to full digestion via aqua regia extraction or, in the case of Sb, were just above the three times detection limit cut-off, and so the reported 0.7 ppm compared to 0.4 ppm CRM is probably acceptable. Aluminium and K are known to be problematic for accurate determination with the UltraFine+™ method, possibly due to partial digestion of the clay, and are of limited use.

Elements that were all close to, or below, the detection limit included Bi, In, Re, Hg, Ta, Te and W. These elements were also at similar concentrations in the full dataset and are not used further.

The half absolute relative difference (HARD: Stanley & Lawie 2007) was calculated as a percentage for all analytes using duplicate samples:

$$\text{HARD} = \left(\frac{\text{assay 1} - \text{assay 2}}{\text{assay 1} + \text{assay 2}}\right) \times 100$$

Laboratory duplicates were analysed at a rate of one per 20 samples to assess precision, and all elements achieved the <20% HARD criteria above. All elements except Al, Ga, Ge, Hf, Sr Ti and Zr were <10%. Gold, unexpectedly, showed more variance if the samples near detection limits were included (HARD > 40%). Commonly, QAQC (Quality Assurance/Quality Control) does not assess results less than five or 10 times the detection limit due to the variance in most techniques, even though the UltraFine+™ results for Au had previously been much better in other testing (Noble *et al.* 2019). Many duplicates were close to the detection limit and when restricted to the samples that were three times the detection limit or more the HARD was 28%, with one sample skewing the data (a duplicate of 17.6 and 2.3 ppb). With this outlier excluded, the results were an acceptable 12% HARD.

Results and discussion

Sir Samuel/Leonora region

The region has numerous Au deposits and the results showed that only 8.8% of the data in the <2 µm fraction was below detection for Au (Table 2) compared to 74% of data for the historical analysis of this same material. Both datasets have similar lower limits of detection (LLDs) for Au (0.5 ppb for this work and 1 ppb for historical data). The GSWA size fraction for analysis was 2000–450 µm using Fire Assay-ICP-MS.

Gold in the <2 µm fraction ranged between 0.5 and 17.6 ppb, with mean and median values of 2.36 and 1.8 ppb, respectively (Table 2). The proportion of censored data was greater than expected given the past samples and test work in other regions by Noble *et al.* (2013, 2019), but is better than the historical data (Fig. 5). The distribution of Au depicts a number of the major mineralized areas effectively, and shows areas like Tarmoola–King of the Hills (Fig. 6) to be prospective with 5.4 ppb Au being 11 times the detection limit and >95th percentile, whereas the previous data from Bradley *et al.* (1995) was 1 ppb, the detection limit and 70th percentile (Fig. 7). The results show the Mt McClure region in the Yandal greenstone belt is elevated with respect to Au (concentrations >5 ppb). The results do not highlight the Bronzewing deposit as much as expected. The area is certainly prospective with consistent Au above 1.5 ppb, but no greater concentrations like those observed in the Agnew–Lawlers area. The data are somewhat noisy as not all samples were anomalous (>5.46 ppb: Fig. 5; Table 2) near major Au deposits. The historical GSWA results failed to show Bronzewing as a target (Fig. 7). The major Agnew–Lawlers Au camp is the largest and also the one that is most prominent in the both soil datasets (Figs 6 and 7).

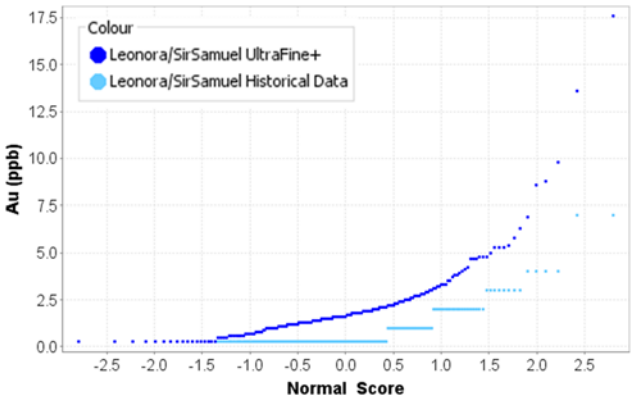

Fig. 5. Probability plot showing the Au data from the UltraFine+™ method and the historical data from Bradley *et al.* (1995) and Kojan *et al.* (1996).

An additional value-add for the UltraFine+™ package is the ability to measure Pt in these soils. The quality control data indicate that the Pt measurements are robust, even though most concentrations are only one–five times the detection limit. In this part of the Yilgarn Craton, Pt may be a useful pathfinder for Ni. Nickel is abundant in the Agnew–Wiluna greenstone belt: for example, Leinster and Mt Keith are world-class deposits in the region. The sampled regional map areas did not focus on Ni, so there is not a great overlap with major deposits (not shown). The marked improvement from the percentage censored data (below detection) in the analysis of both the Leonora and Sir Samuel map sheets was 13.5% using the new method compared to 75% in the previous work with the same samples (Table 2) (Bradley *et al.* 1995; Kojan *et al.* 1996). The Pt concentrations are still very low, with a mean of 2 ppb, a maximum of 5 ppb and a 95th percentile value of 4 ppb.

Cadmium is a problem for the new method and its analysis has been a problem in the past. Many of the data (46%) were below detection limits and if Cd is deemed the best pathfinder element for a specific type of deposit, the UltraFine+™ method may not be appropriate. The region has a very much lower natural abundance of Cd (Table 2) (Bradley *et al.* 1995; Kojan *et al.* 1996).

Silver should also be an effective trace metal of interest that will be extracted by the UltraFine+™ method. Noble *et al.* (2019) tended to focus on Au, Cu and Zn analyses, and Ag was not tested extensively, partly because the results for the soils studied in that publication and in these regional results were all close to the detection limits, although there were no censored data. The precision was very good between duplicate samples (HARD = 3.2%), and again there was a dramatic improvement over earlier analyses that had 67% of Ag data censored using the same materials (Table 2) (Bradley *et al.* 1995; Kojan *et al.* 1996). The distribution of Ag in the region does not add a lot of value for exploration. Many of these orogenic deposits are not Ag-rich, so the mapped Ag-poor results are an accurate reflection of this mineralization style. The mobility of Ag in these environments is commonly decoupled from Au during supergene processes (Anand & Butt 2010) and, as a result, Ag is not an effective pathfinder. It would be of interest to test the UltraFine+™ method on regional soils in an area that has traditionally used Ag as a successful pathfinder or target element.

The censored data of Au, Ag, Pt and Cd will continue to be a challenge for many geochemical soil samples, especially in the transported cover that is abundant in Australia. Slight improvements to the UltraFine+™ method are expected, and there is also potential for improvements to be gained in ICP-MS technology. High-resolution instruments will become increasingly available for standard testing, such as acid digestions of soils. The challenge is

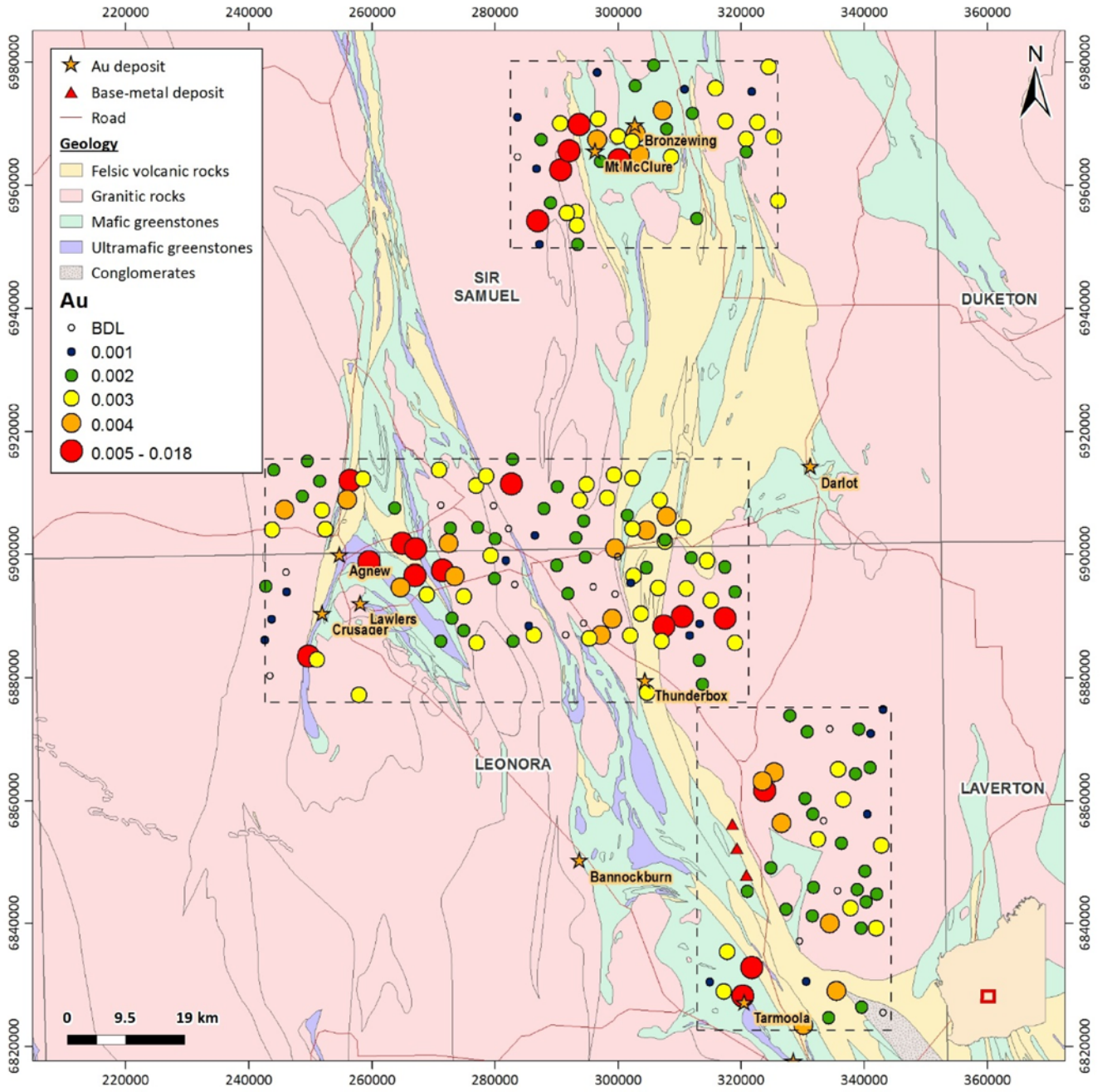

Fig. 6. Gold (ppm) in the <2 µm fraction from archived regional soil samples around significant Au mining areas in the Leonora and Sir Samuel 1:250 000 map sheets. Geology is generalized and based on the data from GSWA (2014). BDL, below detection limit.

to reduce the TDS of the analytical solutions while retaining the low-level precious metals.

Siderophile elements like Cr and V, and, perhaps, to a lesser extent Ni, show the greenstones through the cover. This trend was noted in the earlier published work by GSWA (Bradley *et al.* 1995; Kojan *et al.* 1996) and has since been observed in groundwater geochemistry for this region as well (Gray *et al.* 2016). Chromium and V have similar concentrations in the <2 µm fraction chemistry, with Cr and V mean concentrations of 130 and 135 ppm, respectively (Table 2). The spatial distribution of these two mafic/ultramafic rock indicators is not the same, and high Cr reflects ultramafic rocks compared to mafic rocks: for example, high Cr over ultramafic SW of Agnew (not shown).

Lithophile elements do not add a lot of value to assessing the exploration potential for Au and base metals in the areas tested.

In contrast to the association of siderophile elements and lithology that has been well established, yet only briefly explored here, chalcophile elements show little relationship with lithology in most cases. Silver was discussed previously and is quite uniform across the region; Cd is below detection and Bi is also inconsistent and at low concentrations. The historical samples also showed that 41% of sample results for Bi were censored. For the <2 µm soil fraction, Bi concentrations ranged between 0.2 and 1.3 ppm with a detection limit of 0.1 ppm, and 0% of samples below detection (Table 2).

Copper and Zn results are elevated in the areas of base-metal deposits in the study area, but are not highly anomalous. These elements tend to be variable in these soils, partly due to the scavenging of these elements by variably abundant secondary Fe and Mn oxides. Adjusting data using other parameters related to these oxides will improve exploration targeting, but was not tested here. As noted by Noble *et al.* (2019), there is a significant upside for Au using the <2 µm fraction, but Cu and Zn are also effectively measured in the silt-sized fraction. As a result, the concentrations in

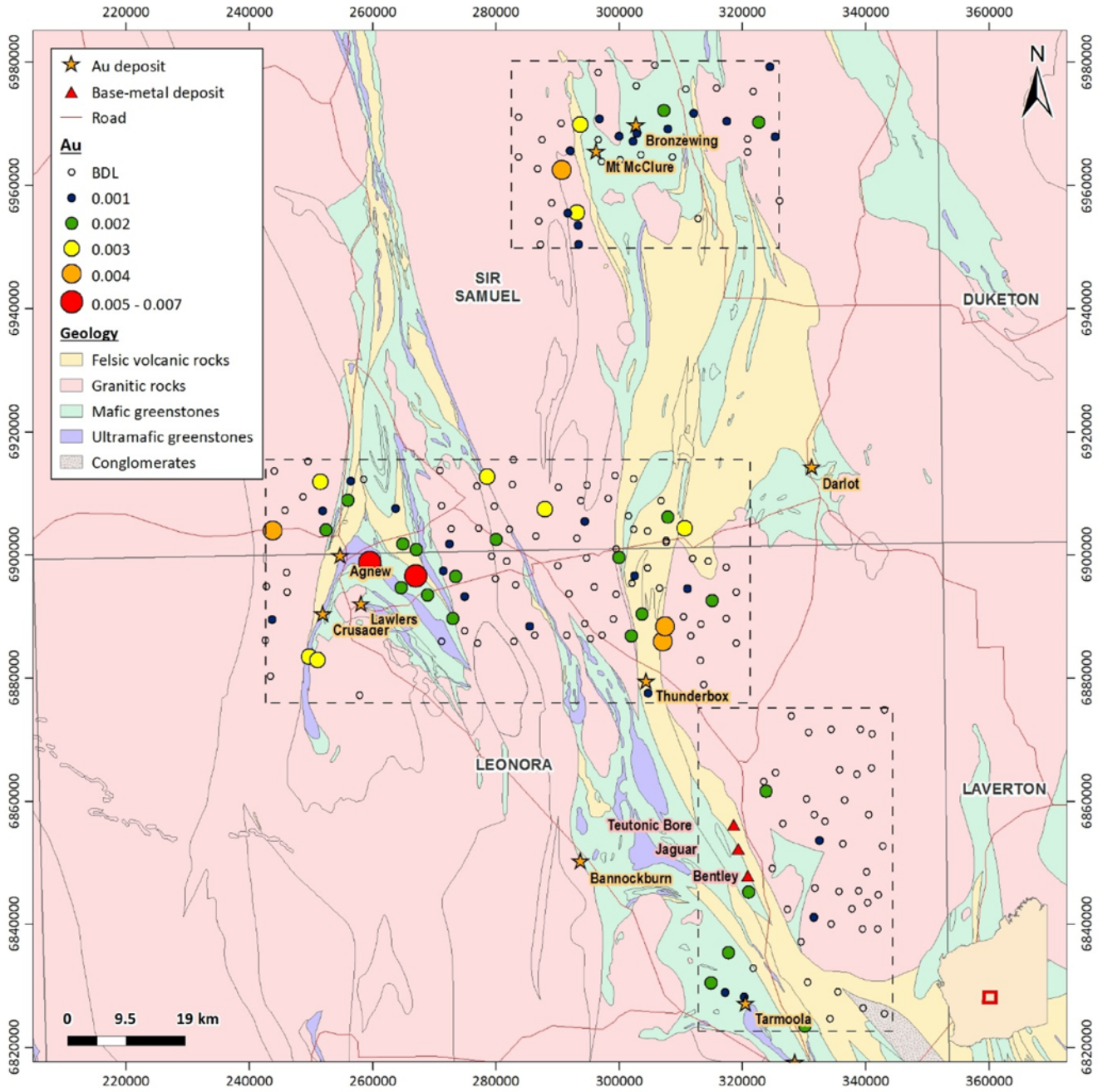

Fig. 7. Gold (ppm) in the archived regional soil sample data from Bradley *et al.* (1995) and Kojan *et al.* (1996) in the Leonora and Sir Samuel 1:250 000 map sheets. Refer to Figure 3 for the names of deposits. Geology is generalized and based on the data from GSWA (2014). BDL, below detection limit.

the finer fractions are greater than the historical data, but the patterns for exploration targeting are similar. The sample <1 km to the south of the Bentley Zn deposit is in the highest quartile, but not the largest concentrations measured.

The Leonora/Sir Samuel results show significant value to improving the results of historical samples. It also suggests that clusters of elevated Au or other target and pathfinder elements are prospective on a regional scale.

Kingston region

The Kingston region is a greenfields exploration area and, although taking in the northern margin of the highly prospective Yilgarn Craton, there is only one known Au deposit (Mt Eureka: Fig. 4). Summary statistics of the results of the UltraFine+™ analytical method applied to 300 soils from the region are shown in Table 3.

The results showed that 12.3% of the data in the <2 μm fraction was below detection for Au (Table 3). The historical analyses of the same 302 samples with a similar detection limit (1 ppb v. 0.5 ppb for the current analyses) resulted in 63% of results being below detection, or 191 samples out of 302, providing more limited use in Au exploration. The difference (and benefit of the re-assayed data) is evident in Figure 8 (A v. B).

Gold in the <2 μm fraction ranged between 0.5 and 8.6 ppb, with mean and median values of 1.76 and 1.5 ppb, respectively (Table 3). Censored data were similar to the Leonora/Sir Samuel soil chemistry results, with the overall Au concentrations lower, which was expected given that this is a region of thicker cover. The results of the UltraFine+™ method are a significant improvement on the historical data (Fig. 9).

The initial data only showed a few samples above detection, with the highest value located *c.*10 km south of the only mined Au in the

Table 3. *Summary statistics for the Kingston regional soils using the UltraFine+™ method*

	% Censored	Minimum	Maximum	Mean	Median	SD	95th percentile
Ag	0.3	0.01	0.13	0.03	0.03	0.01	0.05
Al	0.0	30 100	158 000	89 355	88 250	22 117	130 850
As	0.3	1.5	19.4	7.61	7.5	2.27	11.29
Au	12.3	0.5	8.6	1.76	1.5	1.09	3.9
Ba	0.0	25.7	629	108	86.15	79	219.85
Be	0.0	0.5	3	1.43	1.4	0.38	2.1
Bi	0.0	0.2	2.7	0.43	0.4	0.15	0.5
Ca	0.0	163	81 100	1956	1015	5477	4313.5
Cd	85.4	0.05	0.21	0.08	0.06	0.04	0.1875
Ce	0.0	17.5	168	52.18	45.5	21.48	100.715
Co	0.0	2.7	27.9	9.37	8.9	4.36	16.64
Cr	0.0	45	765	89.40	84	44.87	110
Cs	0.0	2	14.2	6.47	6.1	1.73	9.885
Cu	0.0	8.8	67.6	28.82	27.9	7.73	41.01
Fe	0.0	20 400	71 500	53 879	54 400	8609	66 900
Ga	0.0	8.67	47.9	30.23	30.65	5.78	38
Ge	1.7	0.05	0.74	0.34	0.33	0.12	0.54
Hf	0.0	0.02	1.17	0.43	0.42	0.23	0.82
In	0.0	0.03	0.12	0.08	0.08	0.01	0.1
K	0.0	950	19 900	5603	4880	2854	11 325
La	0.0	9.51	93.6	29.97	26.95	11.07	49.725
Li	0.0	7.1	86.5	30.63	29.75	11.22	50.01
Mg	0.0	281	15 200	1889	1300	1910	6109.5
Mn	0.0	92	4160	431.72	317	395.20	1115.5
Mo	0.0	0.6	5.2	1.54	1.5	0.47	2.385
Nb	0.3	0.5	1.5	0.93	0.9	0.15	1.2
Ni	0.0	8	85	22.40	21	8.10	37
Pb	0.0	8.8	42.3	23.25	22.4	5.62	33.785
Pt	13.9	1	4	1.57	1	0.66	3
Rb	0.0	19	118	65.37	63.1	17.21	99.47
S	0.0	84	3590	375	301	366	851.65
Sb	0.0	0.2	1.3	0.50	0.5	0.11	0.685
Sc	0.0	5	25	14.08	14	3.11	20
Se	0.0	0.49	2.23	1.11	1.095	0.22	1.4585
Sn	0.0	1.2	4.3	2.87	2.9	0.48	3.685
Sr	0.0	7.6	162	33.71	27.85	19.54	72
Th	0.0	6.28	41.2	15.86	15.7	3.38	20.385
Ti	0.0	243	927	595	588.5	116	776
Tl	0.0	0.2	0.7	0.50	0.5	0.09	0.6
U	0.0	0.49	9.68	1.87	1.72	0.75	2.9685
V	0.0	43	168	118	121	17	142
W	0.0	0.2	0.6	0.37	0.4	0.06	0.4
Y	0.0	4.5	44.3	15	13.3	7	30.48
Zn	0.0	13.8	175	53	47.65	22	97.365
Zr	0.3	1	35	15	15	8	28
EC	0.0	9.75	3530	91	32.31	311	230.55
pH	0.0	4.08	8.18	4.92	4.745	0.67	6.3595
<2 µm*	0.0	5	81	52	54	16	74
2–50 µm*	0.0	11	86	33	29	14	64
50–125 µm*	0.0	0	11	1	1	1	3
125–250 µm*	0.0	0	2	0	0	0	1
250–2000 µm*	0.0	0	53	13	12	11	32
>2000 µm*	0.0	0	3	0	0	0	1
SSA* ($cm^2\ g^{-1}$)	0.0	697	71 932	35 716	38 326	16 492	57 812
Kaolin abundance	0.3	0.069	0.352	0.227	0.229	0.047	0.305
Ferric oxide abundance	0.0	0.005	0.143	0.085	0.086	0.020	0.114
Hematite/goethite	0.3	890	913	899	899	3	904

Elemental concentrations are in ppm except Au and Pt in ppb. EC in µS/cm. Spectral scalars are standard output, refer to Noble *et al.*, (2019). $n = 302$.
SSA, specific surface area.
*Particle size distribution is for comparison only and currently over-estimates clay and silt %.

area (Fig. 8a). This sample sits on the edge of the greenstone belt. The rest of the survey is not useful for Au exploration if Au is used as the only target element in these soil samples. The re-assayed results are a major improvement, with Au detected in most samples (Fig. 8b). The Au (and Cu) results are commonly lower than those concentrations measured in the <2 µm fraction in the Leonora and Sir Samuel soils (Fig. 10). Given there were a number of deposits in the Leonora/Sir Samuel region that were identified with

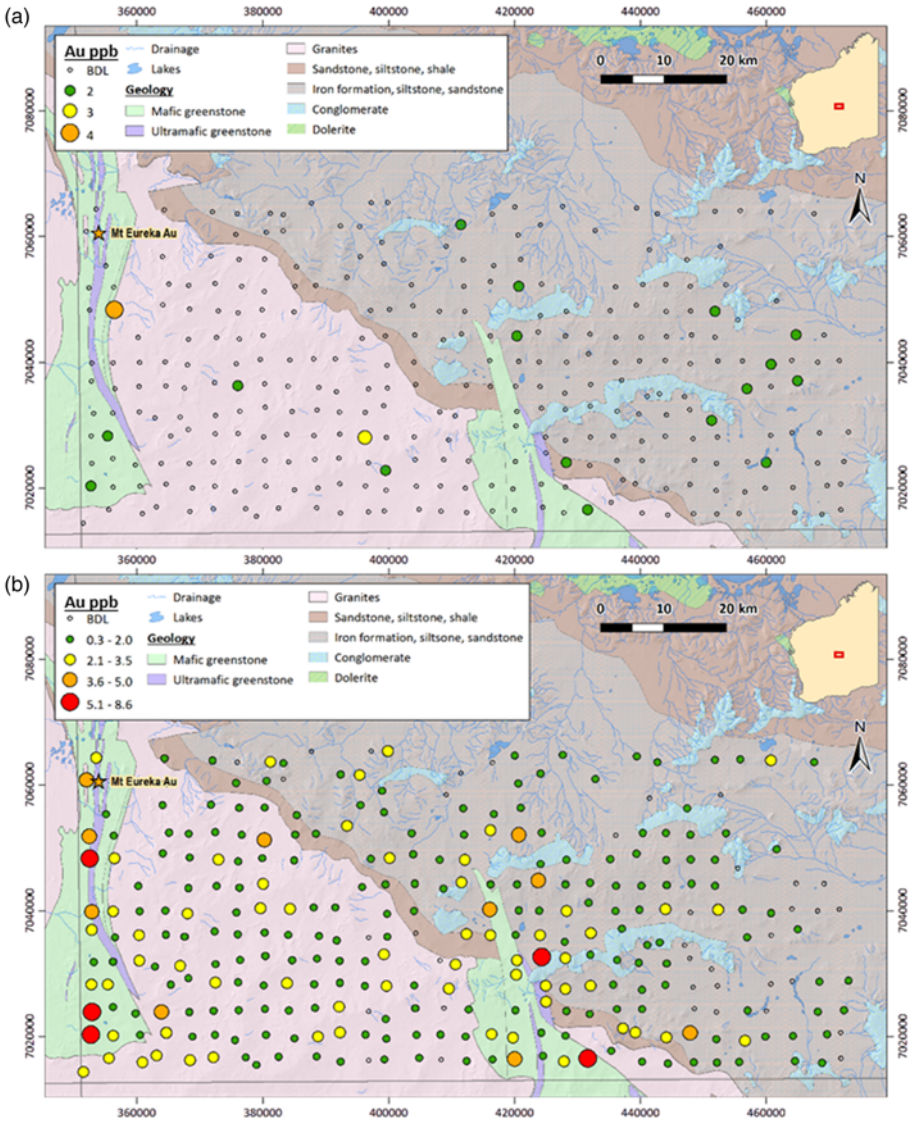

Fig. 8. Gold (ppb) in soils in the Kingston 1:250 000 map sheet. (**a**) Original data with only a few detectable Au values. (**b**) The Ultrafine fractions with natural breaks in scale to better identify anomalous areas. The star represents the (small) Mt Eureka Au deposit. Geology is generalized and based on the data from GSWA (2014). BDL, below detection limit.

concentrations of Au of 3.5–7 ppb (Fig. 6) using the same method, sample sites represented by similar concentrations in Figure 8b are perhaps just as prospective, and clearly much less explored.

As in the orientation regional dataset, Ag and Pt were consistently measured above detection limits using the <2 μm fraction (Table 3), a marked improvement on the past data, with the percentage of censored historical data for Ag and Pt being 64 and 81%, respectively, in the same soils (Pye *et al.* 2000). Even with the additional new data, it is unclear if these elements present additional targets or indicators for mineralization potential in the region. As stated earlier, Ag is not generally associated with Au deposits of the Yilgarn Craton, but potentially may be a more viable target in the basin setting. Platinum changes are subtle and tend to highlight the greenstones in the Kingston region (not shown).

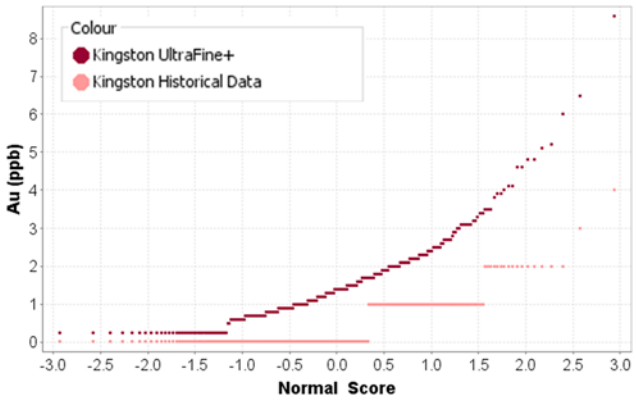

Fig. 9. Probability plot showing the Au data from the UltraFine+™ method and the historical data from Pye *et al.* (2000).

As is observed in the orientation regional sites, siderophile elements Cr, Ni and V (Fig. 11) also tend to occur in greater concentrations in soils that are located near the greenstones. The concentrations of these elements have similar ranges but are about 30% less than those in Leonora/Sir Samuel map sheets, and this is attributed to fewer ultramafic and mafic rocks, as well as the thicker transported cover and increased sandplain areas over the Earaheedy Basin. These mafic/ultramafic rock indicator elements in the soil are in strong contrast to Rb concentrations that map out the basin and sedimentary rocks much more effectively. The Rb is not as high over the granitic rocks as might be expected, and this is postulated to be due to the regolith over the granites being mostly *in situ* and strongly weathered. Some other lithophile elements (e.g. Li: not shown) also replicate this pattern, but not as strongly as that observed in Rb (Fig. 12). Combining these variables in a simplistic additive manner (V + Cr-Rb), as the statistical range of these variables is similar (Table 3), is a very effective way to map the lithology in this region (Fig. 13). Using inverse weighted distances ($1/distance^2$) to extrapolate these data produces an effective map of the Yilgarn Margin into the Earaheedy Basin under cover (Fig. 13).

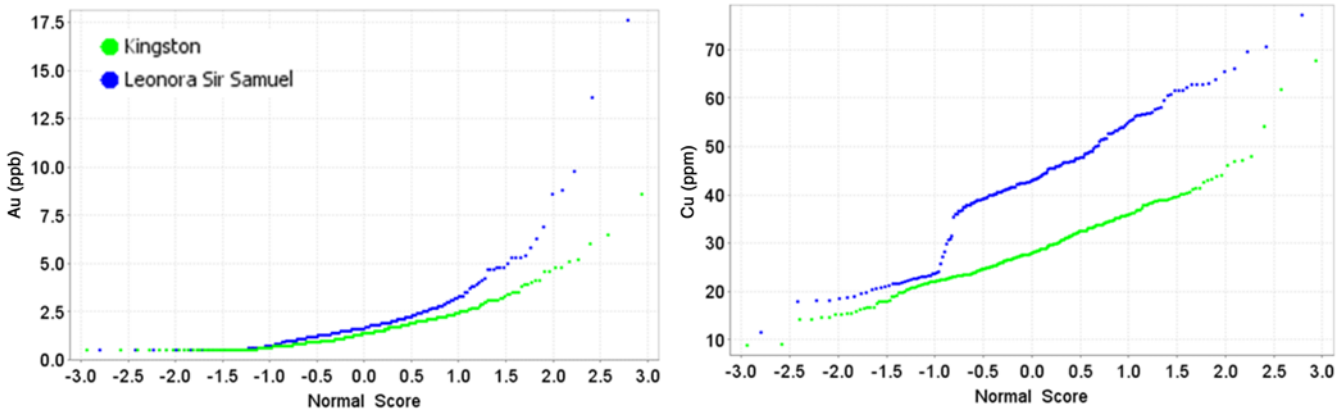

Fig. 10. Probability plot comparing Au and Cu concentrations extracted using the UltraFine+™ method in the <2 μm fraction for both the Leonora/Sir Samuel and Kingston map sheets.

A strong anomaly is present in the SW corner of this lithology additive index map that is attributed to an extreme Cr concentration (765 ppm, 99th percentile) with very low Rb (23 ppm, 1st percentile). This could be a sliver of unmapped greenstone in the Yilgarn Craton, but it is less common that it does not show in the magnetics image (Fig. 13). The supressed magnetic signature could relate to unserpentinized ultramafics that will not have a strong magnetic response without the formation of more magnetite (Toft *et al.* 1990). This change in Fe mineralogy in the lithology is not evident in the UltraFine+™ chemistry. This sample has some Au (2.9 ppb, 87th percentile), but is not anomalous. The Cr concentration is more than twice as much as the next greatest value in the survey (303 ppm).

For exploration purposes, Ni shows a few strong anomalies in a small, clustered area at the edge of the greenstone, which is possibly an extension of the Duketon greenstone belt that has a number of small, Ni deposits associated with it (e.g. Rosie, C2: Godel *et al.* 2012). The historical soil Ni data (Pye *et al.* 2000) show a very similar patterns to those determined using the <2 μm fraction and the UltraFine+™ method (Fig. 14).

In contrast to the association of siderophile and lithophile elements, chalcophile elements show little relationship with lithology in most cases, with a number of these elements poorly extracted using the UltraFine+™ method. Arsenic, Bi, Cd and Se are all close to detection limits (Table 3). Cadmium was rarely detected. Others such as Ga, Ge (and W) have been shown to have poorer reproducibility and some association with Ti and Si, and were not used. These elements are commonly associated with resistant minerals and are incompletely digested (Noble *et al.* 2019).

Base metals such as Cu and Zn tend to be slightly elevated along the greenstones, but also show higher concentrations in the soils in

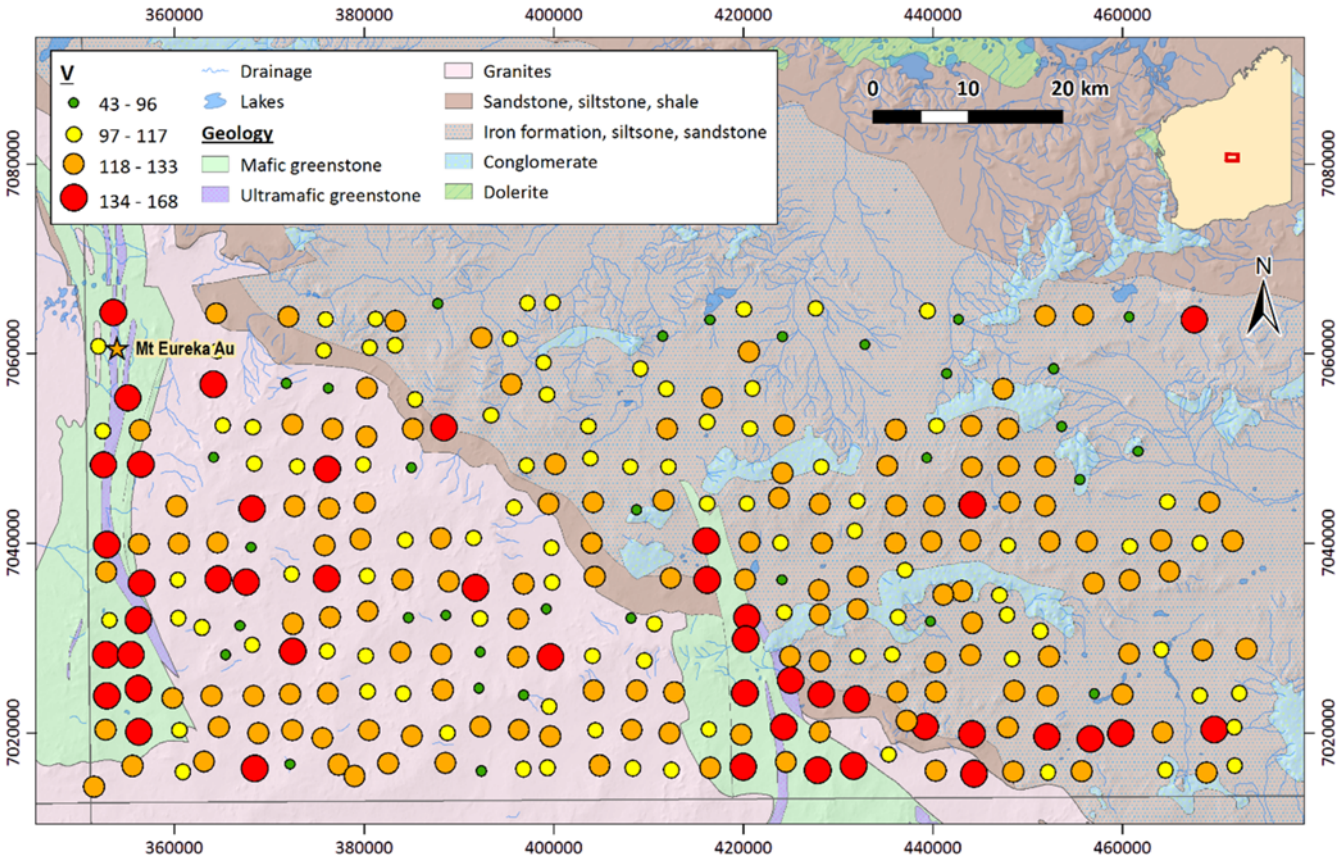

Fig. 11. Vanadium (ppm) in the <2 μm fraction from archived regional soil samples in the Kingston 1:250 000 map sheet. Geology is generalized and based on the data from GSWA (2014).

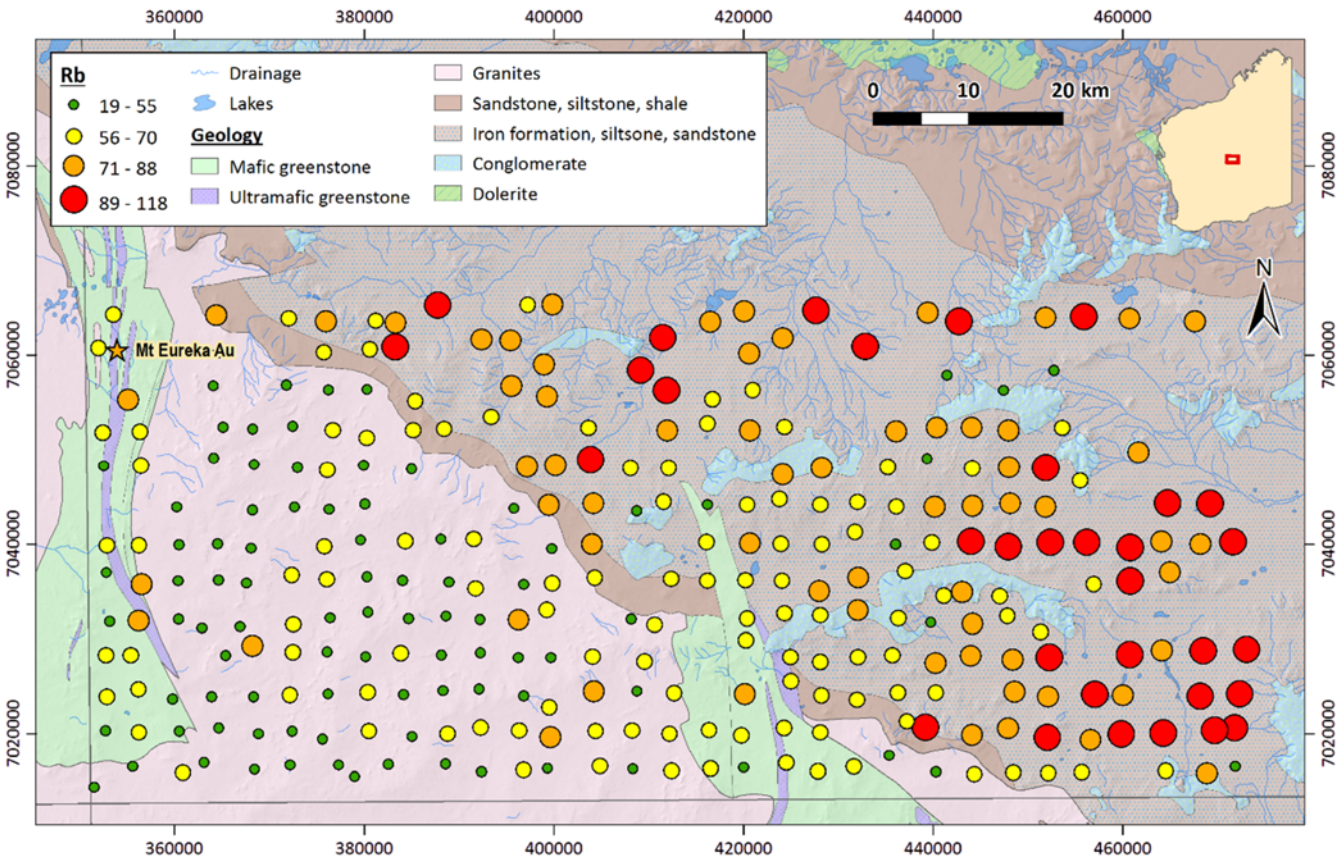

Fig. 12. Rubidium (ppm) in the <2 µm fraction from archived regional soil samples in the Kingston 1:250 000 map sheet. Geology is generalized and based on the data from GSWA (2014).

the basin. The historical data show lower concentrations than the <2 µm fraction results in general. This is evident comparing the plots with the same scale (Fig. 15a and b). The rescaled newer data compared to the old data (Fig. 15a and c) show a more consistent background Cu concentration across the Kingston area. The Cu results perhaps highlight some additional areas with higher Cu in the basin setting (central north and far east), but these are far from anomalous concentrations. Copper correlates with Sc ($R = 0.71$ and 0.85) in both Kingston and Sir Samuel Leonora, respectively, and are likely to reflect a broad lithological control. A weak positive trend is associated between Cu and Zn. Zinc shows similar results with respect to a comparison with older data and the results also tend to show more a background response (Fig. 16). The <2 µm fraction extracts more Zn, yet it does not show more anomalous results than the traditional extraction and analysis conducted in 2000 by GSWA (Pye *et al.* 2000).

Telfer West prospect

The two soil sample lines completed at Telfer West were compared to the nearby drilling data that included composite downhole geochemistry and geology logs. The cover is *c.* 50 m above the weak supergene Au mineralization in the oxide zone. Other target elements of interest that are somewhat enriched at depth include As, Bi and Co. The highest As (11–12 ppm) concentrations in the fine fraction align with the more As-rich oxidized Proterozoic rocks below from drilling data using the surface soils analyses (drill holes ETG 0029 and 0030: Fig. 17). The lowest As concentrations are 7 ppm. The As concentrations for all samples are essentially background. Bismuth is also a vector element at this prospect, but the Bi data in the <2 µm fraction was at the detection limit and not used. Gold concentrations in the surface soils are very low, with the highest value being 2.7 ppb. No clear evidence exists to link the surface expression to Au at depth, and the cover is thick in this region (50 m).

Cobalt, Cu, Ni, Pb, Rb and K all are at their highest concentrations towards the southernmost part of the survey (Fig. 17). The elevated values are not anomalous with the range of Cu 22.4–35.5 ppm being essentially background values for soils. These parameters also correlate with the spectral response of the hematite/goethite ratio, providing additional information from the UltraFine+™ method to assess these values that would not be available from standard geochemical assays. The congruent increase in K may be indicative of changes in clay composition. The spectral response of an absorption feature around the wavelength of 2235 nm (2250d in the UltraFine+™ data output), detected using an algorithm that extracts the depths of absorption features near 2250 nm, is potentially related to Fe substitution into kaolinite or the presence of chlorite (Scott *et al.* 1998; LeGras *et al.* 2018; not shown). This other 2250d parameter also provides evidence of a potential change in clay composition. In general, this indicates that this elevated southern soil chemistry may be a false positive, just a soil type transition, and not a location to prioritize for follow-up sampling. This site highlights the value of the addition of spectral scalars to assist the geochemical interpretation, even though it does not clearly 'see' through cover. The subtle changes in clay type from changes in landscape and/or regolith are then reflected in subtle geochemical changes; all of which may not be noticed by the field technician collecting the soils and not available for the interpretation of the multi-element data. The higher elemental values for Co, Cu, Ni, Pb, Rb and K are in the thickest cover of the region (nearly 80 m, log from ETG0028). Adjusting the results for

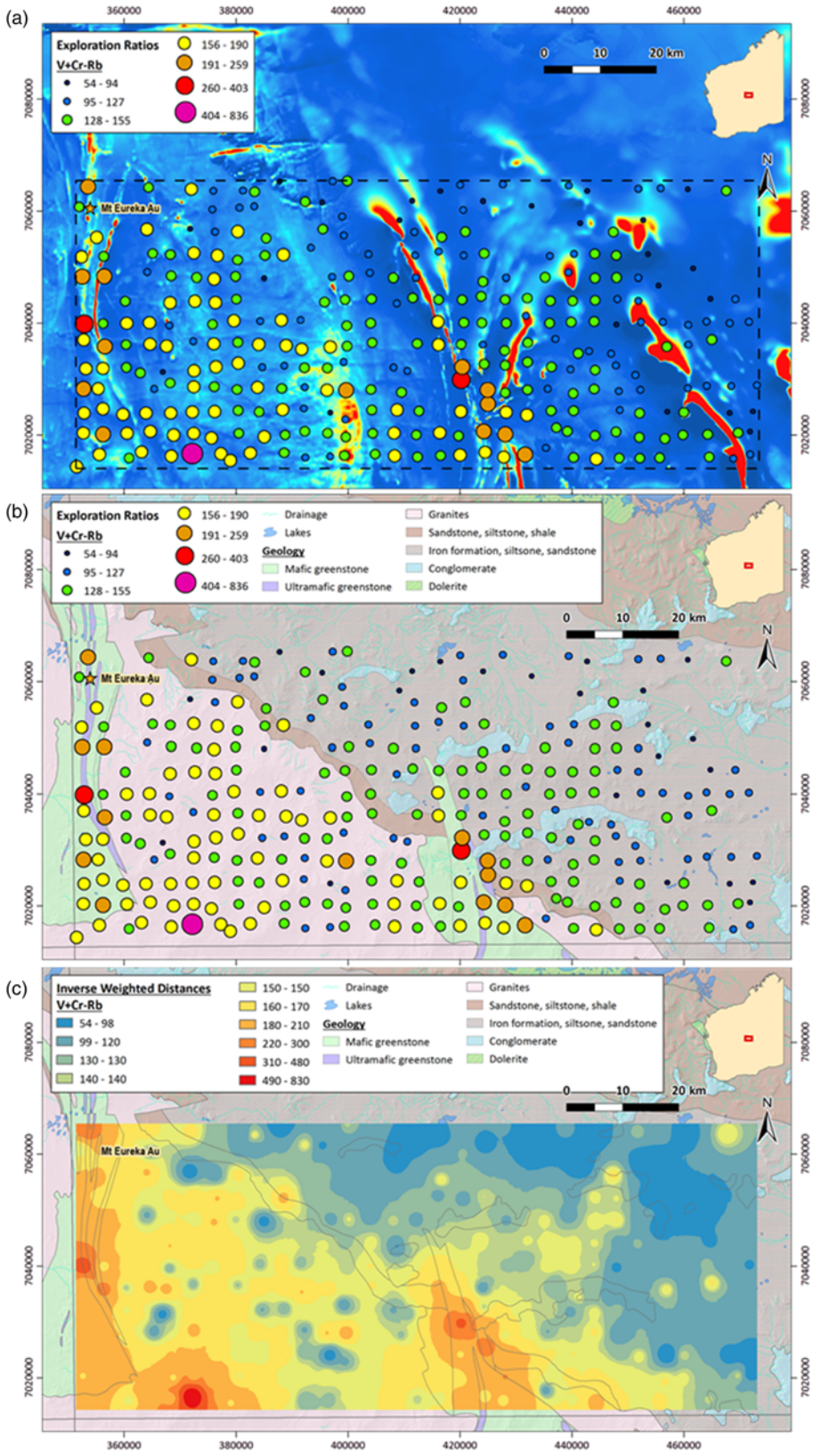

Fig. 13. (**a**) Lithology additive index using V, Cr and Rb data from the <2 µm fraction analysis shown over the magnetics. (**b**) The additive index over the geology map. (**c**) The inverse weighted distance interpolation of these data and the outlines of the major geology units underneath showing a very close association. Geology is generalized and based on the data from GSWA (2014).

the hematite/goethite shift suppresses these values somewhat, further enhances the results for S and Sb, and appears to broaden the Sb dispersion at surface (Fig. 17). The S and Sb results were the only distinctive results in the UltraFine+™ soil data at this site. Many pathfinder elements (e.g. Cu, Co, Zn, Pb) have the greater concentrations in the same southernmost samples, but Sb and S were distinctly different, with their greatest concentrations in the central samples that most closely align with the potential mineralization (drill hole ETG0027). Antimony in these soils is not highly anomalous. It is also not clearly anomalous in the limited downhole, whole-rock geochemistry available. Presently, this appears to be a weak concentration gradient at the surface and it is uncertain if it is related to mineralization.

Tooting Bec prospect

Tooting Bec is a prospect that probably best represents exploration soil sampling in the southern Yilgarn Craton. The underlying

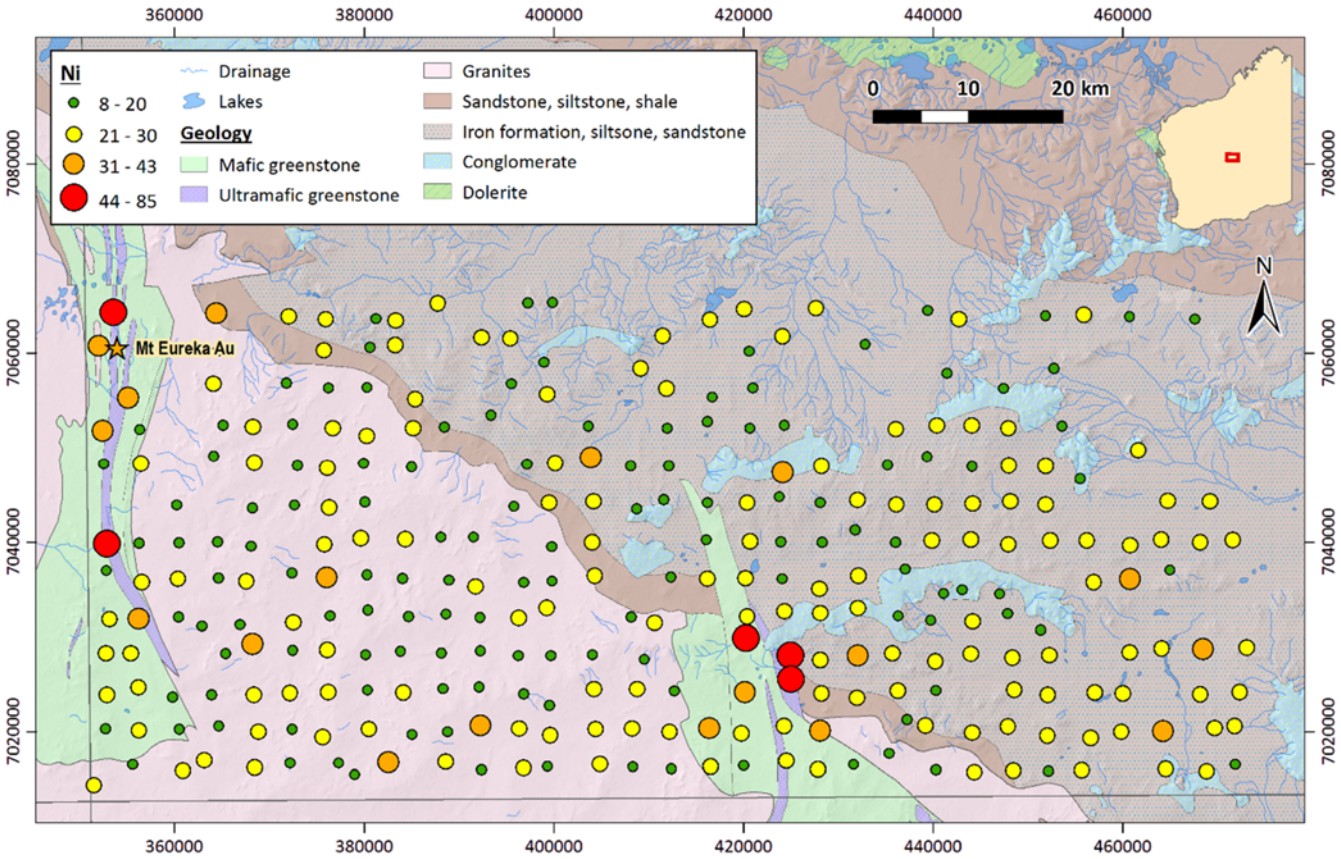

Fig. 14. Nickel (ppm) in the <2 µm fraction from archived regional soil samples in the Kingston 1:250 000 map sheet. Geology is generalized and based on the data from GSWA (2014).

mineralization was not well defined at this site, but the central section of the survey area was the target area. This site specifically looked at the comparison of three size fractions: <2 µm, <250 µm and <2000 µm.

Other studies have shown that coarse pisolitic lag can sometimes be an effective sample media in the Yilgarn Craton, and concentrate Au particularly in the cortices of the pisoliths (Anand & Butt 2010; Anand *et al.* 2016*b*). At Tooting Bec, however, the fine fraction consistently had much greater Au concentrations of *c.* 250% more (Fig. 18).

The average HARD for Au was 5% in the <2 µm fractions and no samples were below detection or close to the detection limit of 0.5 ppb (Fig. 19). The Au concentrations in the <2 µm fractions at this site range from 10.3 to 175 ppb with a mean of 59.5 and a median of 53.4 ppb. The box plots do not show the individual sample comparison, and Figure 18 better shows this comparison at each sample point. The pattern is very consistent and obvious for Au. Arsenic, another common pathfinder in this region, is also slightly greater in the <2 µm fraction. For Cu and Zn the fractions seem similar, which was observed in the method development (Noble *et al.* 2019). Although similar, the coarse fraction tends to have slightly more Cu and Zn in the selected samples.

Iron and Mn oxides can influence trace metal distributions, and have been used as target phases for partial extractions (Chao & Zhou 1983; Hall *et al.* 1996). The results at this site show that Mn (Fig. 20) and Fe (not shown) do not vary much in the <2 µm fraction and do not have a relationship with Au. As the size fraction increases, the Mn (and Fe) concentrations vary much more. Iron or Mn are sometimes used as an element to level data (Anand *et al.* 2007; Noble 2012), and these results show that the UltraFine+™ method would not require this adjustment and performs potentially better than the coarser fractions at Tooting Bec.

Fine fractions of Au (and Cu and Zn) are anomalous over the central region and represent the most prospective target (Fig. 21). This finding is similar in the other fractions too, although concentrations are not as high so there is less contrast in the coarser fractions. The greatest Au concentrations in the soils at Tooting Bec trend in a NW–SE direction and may be influenced by the gently sloping sheetwash plain that slightly offsets the anomaly from the inferred strike of mineralization, which is believed to trend more north–south in the central section of the soil survey. With limited additional site data at present, the <2 µm fraction analysis performs better than the other two size fractions for the geochemistry alone.

DeGrussa deposit

The DeGrussa site was previously sampled, analysed and reported by Noble *et al.* (2017), who were investigating a variety of sample media and the mechanisms of metal migration at this site. Soil orientation traverses used the coarser <250 µm fraction and aqua regia extraction, which is directly comparable to the <2 µm UltraFine+™ extraction method, with the main difference being the sample grain size. The comparison test shows that both extractions effectively identify the mineralization using both Au and Cu (Fig. 22). The concentrations extracted in the <2 µm fraction are greater and the size of the anomaly a bit wider, making it arguably a better method (Table 4; Fig. 22). The increased size of the anomaly more closely matches the dispersion model suggested by Noble *et al.* (2017) where Au was mobilized in the lateritic materials towards the palaeochannel to the north and outside the oxidized Au zone, whereas Cu was more uniformly dispersed in the clays and Fe oxides, and matched the secondary Cu zone offset towards the south. The <250 µm fraction had slightly more contrast (lower

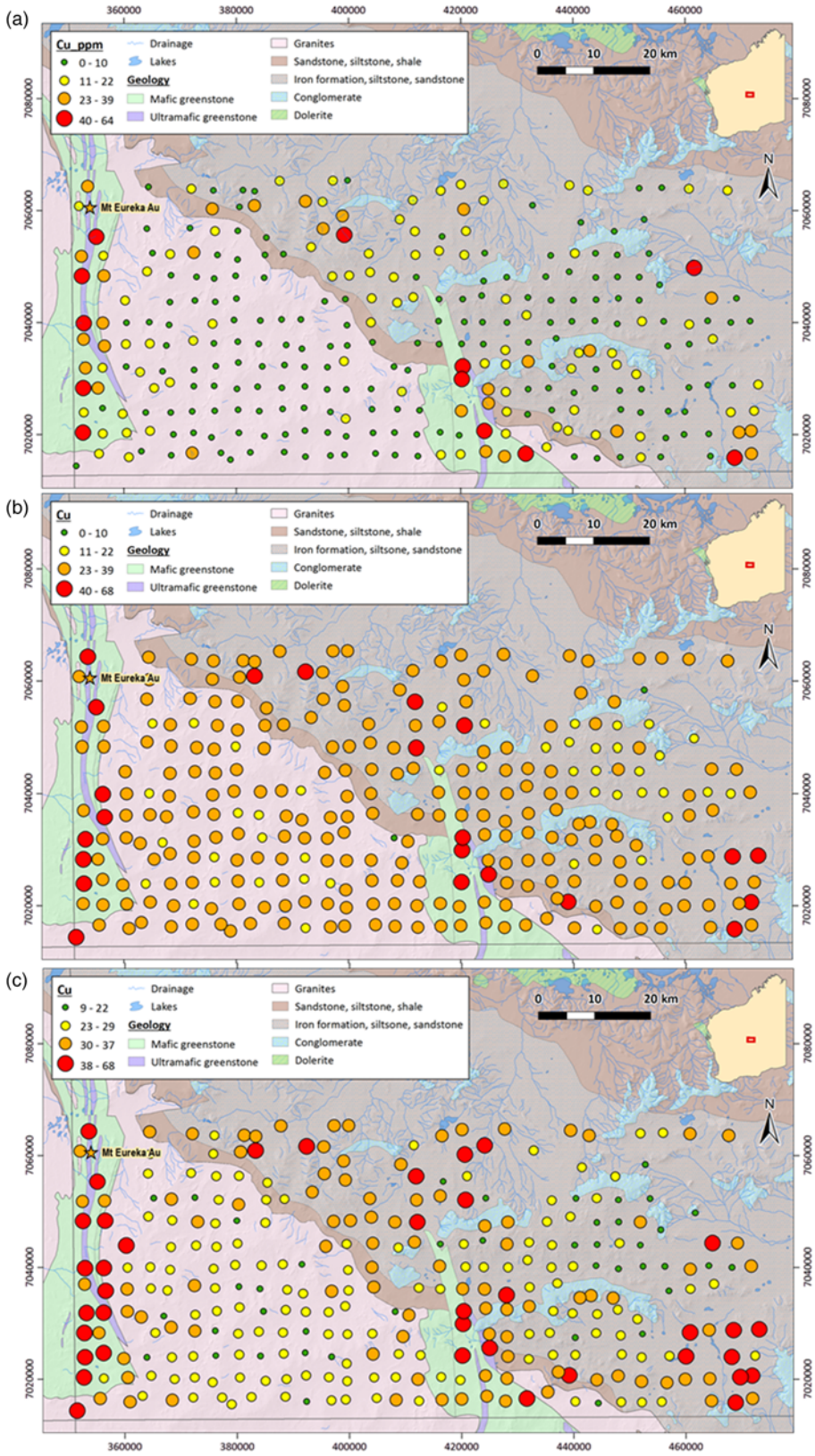

Fig. 15. Copper (ppm), Kingston. (**a**) Historical data (Pye *et al.* 2000). (**b**) The >2 μm fractions of Zn using the same scale as the historical data. (**c**) The >2 μm fractions with natural breaks in scale to better identify anomalous areas.

background) and, in effect, the methods produce very similar results (Fig. 22). The application of the UltraFine+™ method with additional parameters, such as pH, EC, particle size and spectral mineralogy, did not add more to the exploration potential with this first-pass assessment.

The surface signature of the secondary, supergene mineralization at the DeGrussa Cu–Au sulphide deposit is evident in both methods tested and other sample media (Noble *et al.* 2017). The transported cover is shallow here (<10 m), and testing the UltraFine+™ method in the deeper cover (30 m) further south should be considered to test the maximum depth of cover the method may be able to 'see through'. Other studies in this environment and others in Western Australia show a depth of cover limitation to be <10 m (e.g. the Jaguar and Moolart Well deposits) (Anand *et al.* 2007, 2009). During weathering, the Au and Cu have mobilized separately forming different dispersion patterns (Noble *et al.* 2017), and the <2 μm fraction analyses is as suitable as any in detecting this signature.

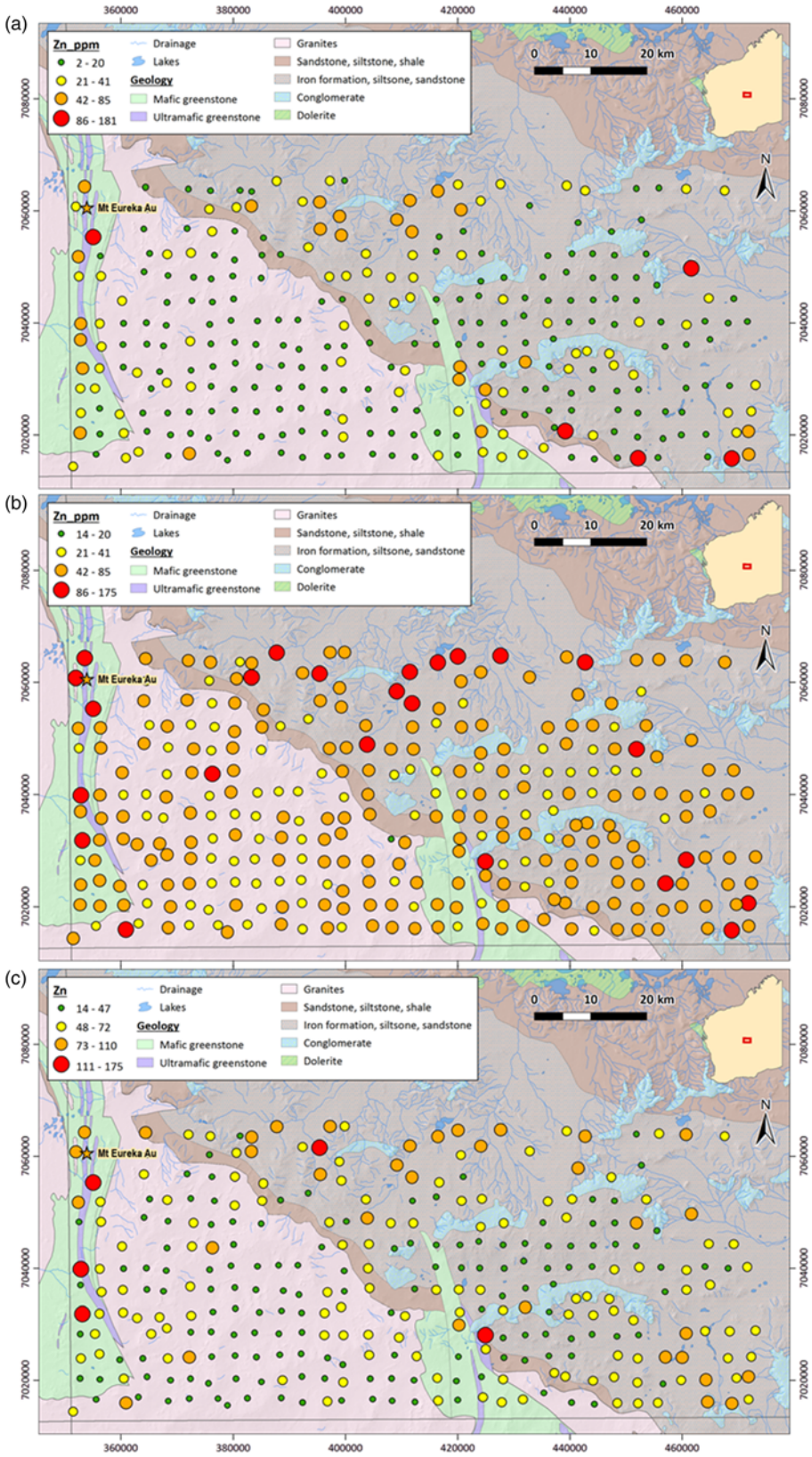

Fig. 16. Zinc (ppm), Kingston. (**a**) Historical data (pye *et al.* 2000). (**b**) The >2 µm fractions of Zn using the same scale as the historical data. (**c**) The >2 µm fractions with natural breaks in scale to better identify anomalous areas.

Other studies and applications related to the UltraFine+™ method

Although focusing on exploration through cover, the application of fine fractions to stream sediment sampling shows the value and confidence in reproducibility that the fine fraction can provide. A Canadian stream sediment survey missed a major opportunity in the analysis of Au, when the reproducibility of the selected analytical method was extremely poor (Arne & MacFarlane 2014). The White Gold region discovery was made using soil geochemistry in an area where the Canadian survey primary stream sediments gave a false negative Au response. The results delayed Au exploration in the region by many years; an area that is now known to host numerous Au deposits (e.g. Coffee) (Wainwright *et al.* 2011; MacKenzie *et al.* 2015). A test of just a selection of these sediment samples shows that reproducibility is poor with a number of other standard methods

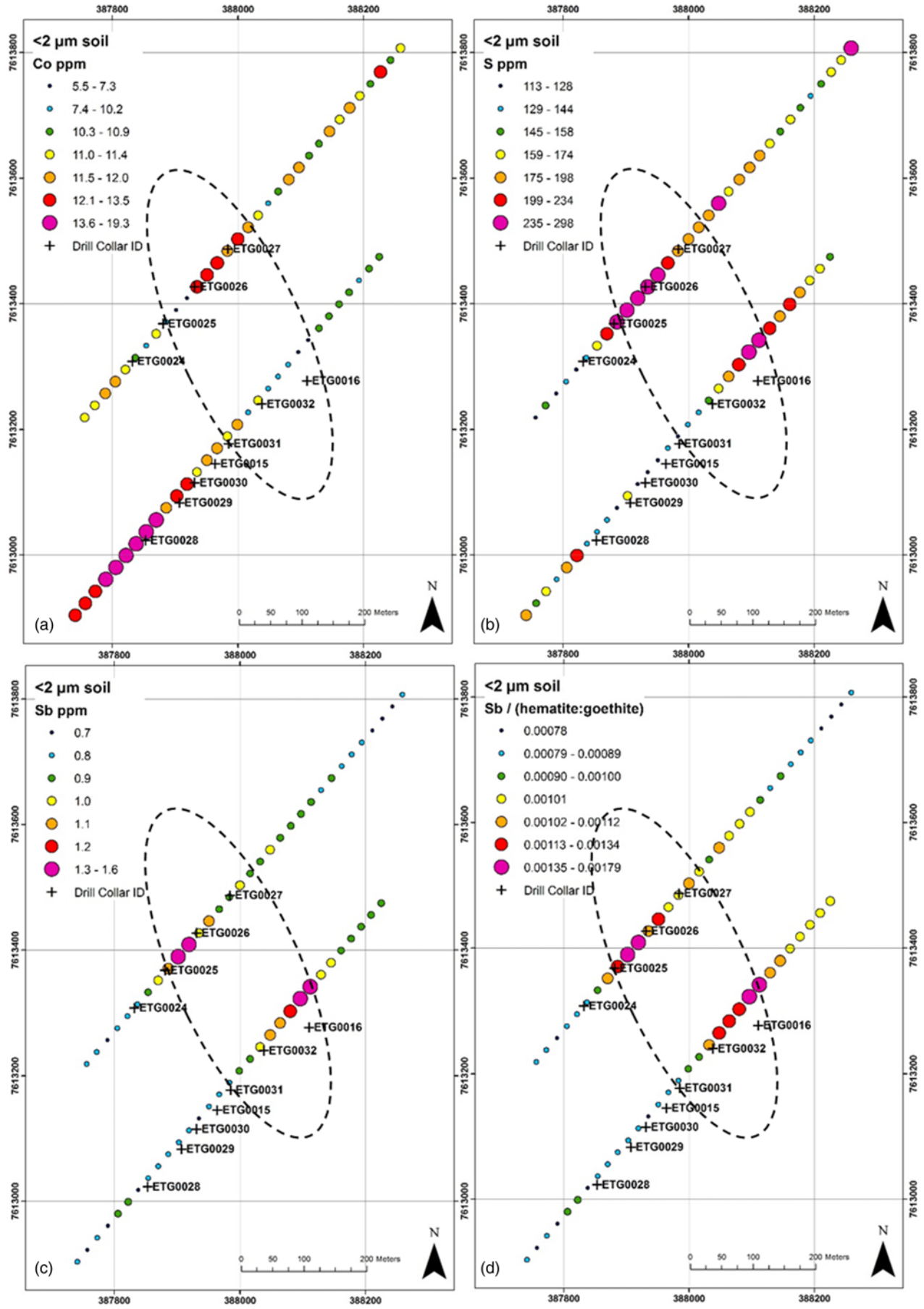

Fig. 17. Surface geochemistry at Telfer West using the UltraFine+™ method. (**a**) Co (ppm). (**b**) S (ppm). (**c**) Sb (ppm). (**d**) Sb adjusted for the change in the hematite/goethite ratio from spectral mineralogy. The dashed black line shows a general location of base-metal and Au mineralization at depth (>40 m).

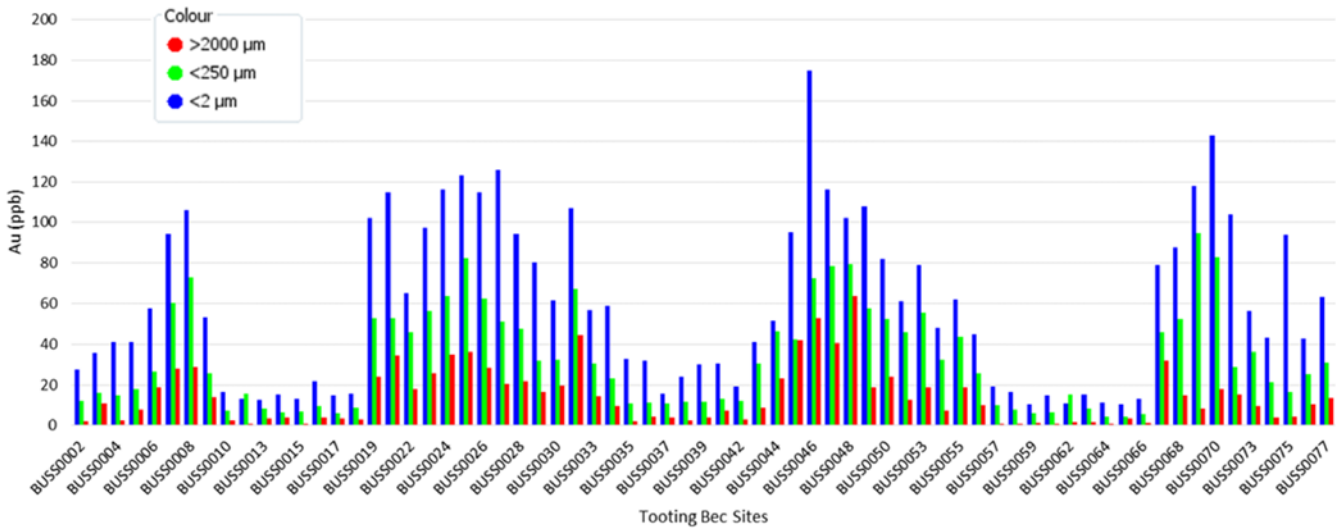

Fig. 18. Individual sample comparisons of Au in the different particle sizes analysed.

used in the industry, such as BLEG (bulk leach extractable gold) or a slightly finer fraction (<177 µm), but the very-fine fraction (<4 µm, mostly clay) produced excellent reproducibility of Au (Arne & MacFarlane 2014). The result demonstrates the immediate impact that improved methods can have on previously collected samples and regional survey data. Although the reproducibility was reasonable (RSD <20%: Pye *et al.* 2000) in the earlier regional survey work by GSWA in Western Australia, the change in the amount of data reported for Au (reduction in censored data) has seen major improvements realized in the samples used as part of this study too.

The preliminary analysis of East Wongatha sandplain soils showed that samples are predominantly coarse material, and initially report Au concentrations of less than detection (0.5 ppb) up to about 30 ppb (Noble *et al.* 2013). Separation and concentration of the <2 µm samples proved the clay fraction contained much more Au and no samples were below the detection limits: that is, in this example there were no censored data. The results of Noble *et al.* (2019) and the results in this paper support the observed increase in concentrations reported by Noble *et al.* (2013), but not to the extent presented in the earlier study that showed an order of magnitude or more increase in Au concentrations. The average increase in Au using the <2 µm fraction in this current and more comprehensive study is of the order of a 150–250% increase. While this is not as great an increase as earlier results had suggested, it is important to recognize that from approximately 1000 different WA soil samples, most from transported cover, <10% were below detection for Au; an exceptionally valuable contribution for exploration soil sample geochemistry in areas of dominantly inert quartz-rich cover. Previous analysis of these soils would have resulted in >70% of samples below detection limit for Au based on the three regional geochemical surveys used in this study (Sir Samuel, Leonora and Kingston: Bradley *et al.* 1995; Kojan *et al.* 1996; Pye *et al.* 2000). These surveys are representative of soils sampled in the northern Yilgarn Craton, the Capricorn Orogen, and various basins to the north and further east in Western Australia where transported cover thickens and becomes a major challenge for mineral exploration. An additional benefit to this reduction in censored Au data is for statistical interpretation, as the method shifts a greater amount of useable geochemical data that is valuable to multivariate analysis options. Previously, the Au results were heavily skewed due to samples being at or below detection limits. This specific issue is further discussed by Leybourne & Rice (2013), albeit for general geochemical data and not fine particle material analysis. The results of the research presented here and in other referenced studies supports the idea that the <2 µm geochemistry significantly reduces the nugget effect, even though precision is not always as tight as expected (Noble *et al.* 2019).

Much like explorers went from single-element assays to multi-element assays, we believe the next decades of exploration will see multi-element data integrated with spectral mineralogy and other parameters as part of the 'standard assessment'. Spectral data were collected extensively in this study, yet has been a lesser component of the evaluation. Like the industry, research is also attempting to catch up with the development of big/more data and how we can best use it.

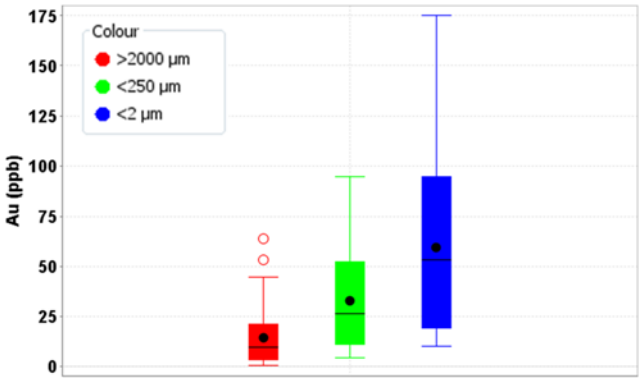

Fig. 19. Box plot showing the data distribution for each of the three separated size fractions at Tooting Bec. The black bar is the median and the black dot is the mean.

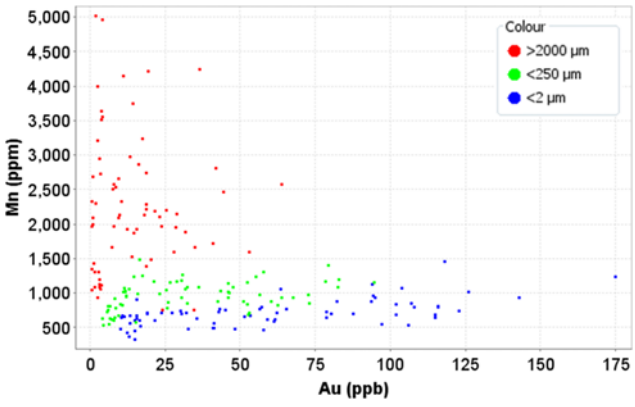

Fig. 20. Gold and Mn scatterplot with results coloured by size fraction.

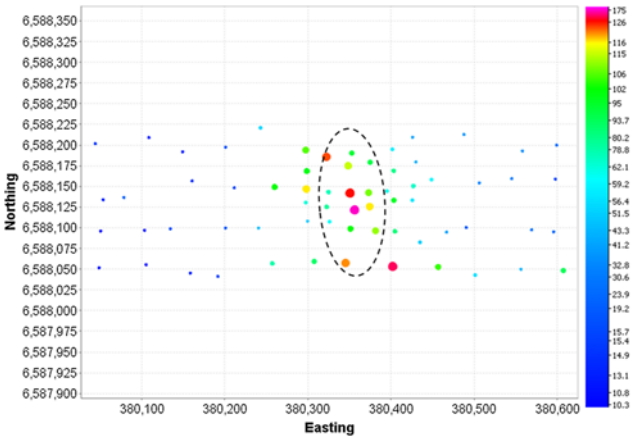

Fig. 21. Gold from the <2 μm fraction at Tooting Bec using the UltraFine+™ method. The dashed line outlines the inferred location of Au mineralization. Concentrations are in ppb.

Spectral data did show evidence of mapping lithology trends in some cases, picking up felsic volcanics in the Leonora map sheet (not shown), but this is likely to be the next progression of this workflow with stronger integration of the 'other' data.

Other data can also map lithological changes and integrating these is important to future applications of exploration geochemistry. Morris (2013) showed some element concentrations in the <50 μm surface soils tended to match up with the aeromagnetic signatures of buried greenstones that extended under cover. The distribution of samples with higher concentrations of fine-fraction Au, Cr and V in soils shows a strong relationship to Yilgarn Craton greenstone belts, which is consistent with the established connection between Au mineralization and greenstones in the Yilgarn Craton (e.g. Blewett *et al.* 2010; McCuaig *et al.* 2010; Morris 2013). The numerous observations of bedrock or even bedrock-hosted mineralization being identified through transported cover (Kelley *et al.* 2003; Wang *et al.* 2007; Morris 2013; Anand *et al.* 2014; van Geffen *et al.* 2015; Noble *et al.* 2017, 2018) does imply some migration of these materials through the cover. It is important to distinguish between geochemical signatures mobilized vertically through transported cover and those similar signatures that could be derived from proximal colluvial/alluvial dispersion. In the soils studied from the Kingston map sheet, drainage is minimal and not related to the lateral transport of greenstone minerals and related chemistry into the soils: that is, coincident shedding of greenstone materials from those belts subcropping out further south is not occurring (Fig. 13).

We see these greenstone extensions in the Kingston map using the <2 μm fraction. These extensions trend north under the Earaheedy Basin and should be considered for future exploration. Major exploration success in recent times in Western Australia has come from explorers stepping out into the lesser known and more covered greenstone belts in Western Australia. The discovery of the Gruyere Au deposit in the Yamarna greenstone belt and the Nova Bollinger Ni deposits in the Albany Fraser region are clear examples of industry successfully pushing into lesser explored terrains. The edges of the Yilgarn Craton, particularly the NE, as investigated in this study are underexplored, prospective terrains. The techniques and results developed in this project should assist more exploration in the Kingston area and other greenfields settings.

Even though a few elements have not really added significant value or change by being processed with the UltraFine+™ method in the Kingston map sheet greenfields setting, there has been no negative impact by re-assaying these samples, with a significant upside for Au. Gold is providing new information and is not associated with any other variable measured. The other major value of the workflow applied here is the additional information provided (including spectral mineralogy and particle-size analysis) that is not routinely used and therefore not intuitively applied. This added value could include mapping the mineralogical alteration halos associated with mineral deposits and regolith material characterization. For example, the assessment of kaolinite crystallinity (2160 nm feature) can be used to differentiate transported from *in situ* weathered saprolite (Haest *et al.* 2012; Laukamp *et al.* 2015), whereas shifts in mineral chemistry in white micas and chlorite minerals have been shown to highlight alteration haloes at the Abra Pb–Zn-Cu–Au deposit in Western Australia (Lampinen *et al.* 2019). The application of kaolinite crystallinity does suggest that slightly more transported material may be present in the Earaheedy Basin compared to the Yilgarn Craton (Fig. 23).

For particle-size data, although the current methodology overestimates the proportion of fine materials, the results provide a variable for comparison; an estimate of cation-exchange capacity of mobile metals which should be used to interpret the regional geochemical patterns. This may prove useful for understanding (false positive) geochemical anomalies in other settings. Results for the Kingston map sheet using the UltraFine+™ method shows that the selected soils have quite a range in their specific surface area (SSA), with a mean of 35 716 $cm^2\ m^{-1}$ and a standard deviation of 16 492 $cm^2\ cm^{-1}$ (Table 3) using the wet separation sample. The SSA is calculated based on the clay particle-size distribution and so the concentrations of clays $\ll$ 2 μm influence this result.

Another major metal-exchange phase are Fe oxides, and the spectral results for Fe oxide abundance are also valuable information for assessing anomalous results. The Fe oxide abundance has a correlation coefficient of 0.68 with SSA, 0.65 with clays <2 μm and 0.61 with clays <0.2 μm. Using SSA or, perhaps, the amount of fine clays (<0.2 μm) may be useful as these will have more exchange surfaces. Ratios of elemental concentrations with the total % clay perhaps have less utility with the UltraFine+™, as the method effectively separates this clay fraction only and, in effect, is levelling all soil geochemical signatures irrespective of the bulk soil clay content. The best algorithms to integrate these data with the geochemistry for exploration are not known, and further testing will assist in refining the method and interpretation. As an example of potential future maps that could be developed using this workflow, we created two example indices. One uses Au in a ratio with SSA, the other is a multi-element (Au, Bi, Cu, Zn, Ni, Pb, Pt) combination that is adjusted for exchange phases (clay and Fe oxide abundance: Fig. 24).

The results of these new maps highlight a potential change in focus for some of the Au regions of interest. In the Kingston area this may not prove that valuable, but could certainly prove effective elsewhere, especially when soil types vary significantly and can create a lot of false positives. The other exploration ratio picks out the Mt Eureka region and the further extent of that greenstone belt which host Mt Eureka as prospective, but it also highlights the western edge of the other greenstone belt in the central south of Figure 24. This area was noticeable in a number of elements (Au, Ni, Pt), so while it may be identified as an area of interest using single elements, there is a lot of potential to use multiple variable and additional information such as particle size and mineralogy proxies to improve exploration and discern false positives (or negatives).

This study, for both regional and site-based orientation, confirms that the finer fraction is providing much more information than previously employed methods. These results are also supported by other research (Wang *et al.* 1995; Robertson 1999; van Geffen *et al.* 2012; Arne & MacFarlane 2014; Carlson 2016; Sader *et al.* 2018). Another demonstrative study published by Anand *et al.* (2014) shows the <53 μm grain-size fraction had much greater concentrations of Au over the Moolart Well deposit, whereas the commonly used <250 μm soils were ineffective, and likewise the results of Morris (2013) suggest a similar size fraction in East Wongatha

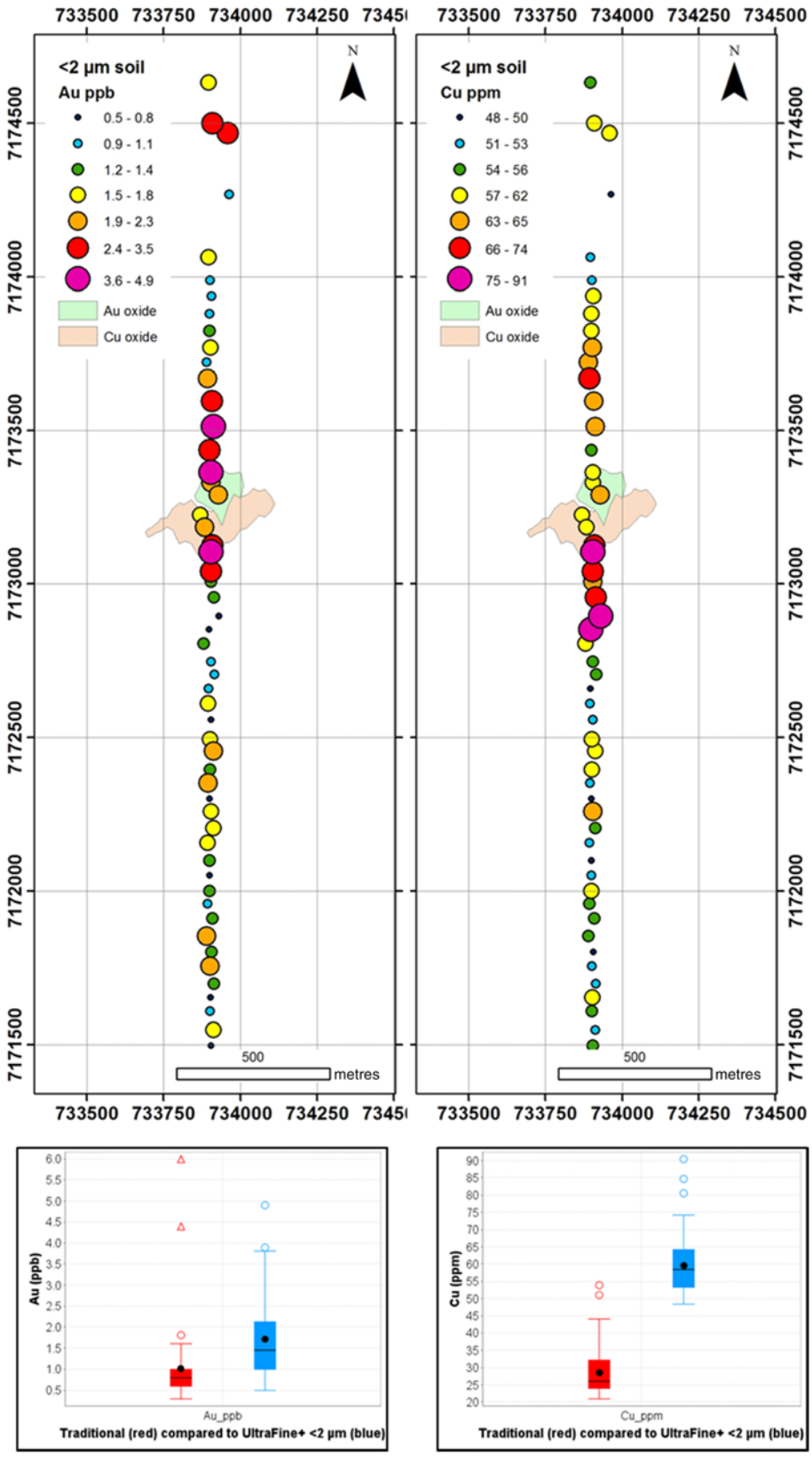

Fig. 22. Orientation traverse at DeGrussa with results for the UltraFine+™ shown for Au (ppb) and Cu (ppm). Box plot inset show the differences in concentrations between the UltraFine+™ and standard aqua regia methods for both elements. The secondary dispersion of ore-grade supergene Au and Cu depicts the mineralized zone.

identified other targets through transported cover. Although not as fine, the <53 µm is an improvement and it seems that the <2 µm is a step change in near-surface exploration geochemistry.

Much of this research has focused on the challenges of Au exploration. The same potential challenges and opportunities are available in exploration for base metals, REE and more, as exploration for these commodities also commonly favours regional soil sampling and geochemistry to refine targets. Recent studies in thick transported cover for base-metal exploration in the Kalahari Desert show the greater metal content is in the fine fractions, with the bulk material showing Pb and Zn concentrations near detection limits and being composed of coarse, aeolian quartz-dominated sands. Analysing fine fractions results in samples that are orders of magnitude above detection limits (Salama *et al.* 2016).

Evidence and examples of the very-fine particle-size geochemistry greatly improving results have been presented, particularly in areas where the amount of censored data is problematic. The question now is: how many similar samples have been overlooked in

Table 4. *Summary statistics*

	Minimum	Maximum	Mean	Median	SD	95th percentile
Aqua regia with <250 µm soil fraction						
Ag	0.006	0.024	0.011	0.01	0.004	0.02
As	3.1	5.7	4.01	3.9	0.55	5.1
Au	0.3	6	1.02	0.8	0.90	2.5
Cu	21	54	28.5	26	7.3	45.8
S	50	400	104.6	50	94.3	362.5
Zn	12	47	19.3	18	6.2	32.3
UltraFine+™ <2 µm soil fraction						
Ag	0.04	0.11	0.054	0.05	0.012	0.08
As	6.1	9.9	8.02	8.1	0.91	9.4
Au	0.5	4.9	1.71	1.45	0.95	3.8
Cu	48.3	90.5	59.5	58.4	8.7	81.6
S	127	1050	445.4	404.5	215.4	895.5
Zn	67.4	350	116.3	103.5	50.3	233.8

$n = 54$, 0% censored. All values are in ppm, except for Au which is in ppb.

bulk analyses by the exploration industry? The immediate impact of the improved methods developed by Noble *et al.* (2019) could be realized by industry and surveys re-testing their historical samples; an immense resource that remains in many industry and government survey storage areas.

As a parallel example, another recent study demonstrated the value of re-assaying approximately 100 regional samples with improved methods for Cu–Au exploration. Baker (2015) showed that the Wafi Golpu area in Papua New Guinea stood out clearly using finer size fractions (<75 µm) and better detection limits with a multi-element anomaly where it was overlooked in earlier sampling and analysis. Not only does this demonstrate the immediate value that can be recognized in re-assaying samples with an improved method such as UltraFine+™, but Baker *et al.* (2015) went further to demonstrate there are more than 10 000 000 samples/geochemical results with open access and there are many times this many samples in archives of industry that could benefit from this type of research and application. The opportunity for industry to regenerate exploration interest using the UltraFine+™ workflow is highly significant, just based on samples in storage alone. However, the industry needs to see the value of such an exercise, and this study has delivered the initial demonstration in areas of cover in Western Australia. It is envisaged that more commercial laboratories will take up this workflow for future offerings to industry to improve mineral exploration globally.

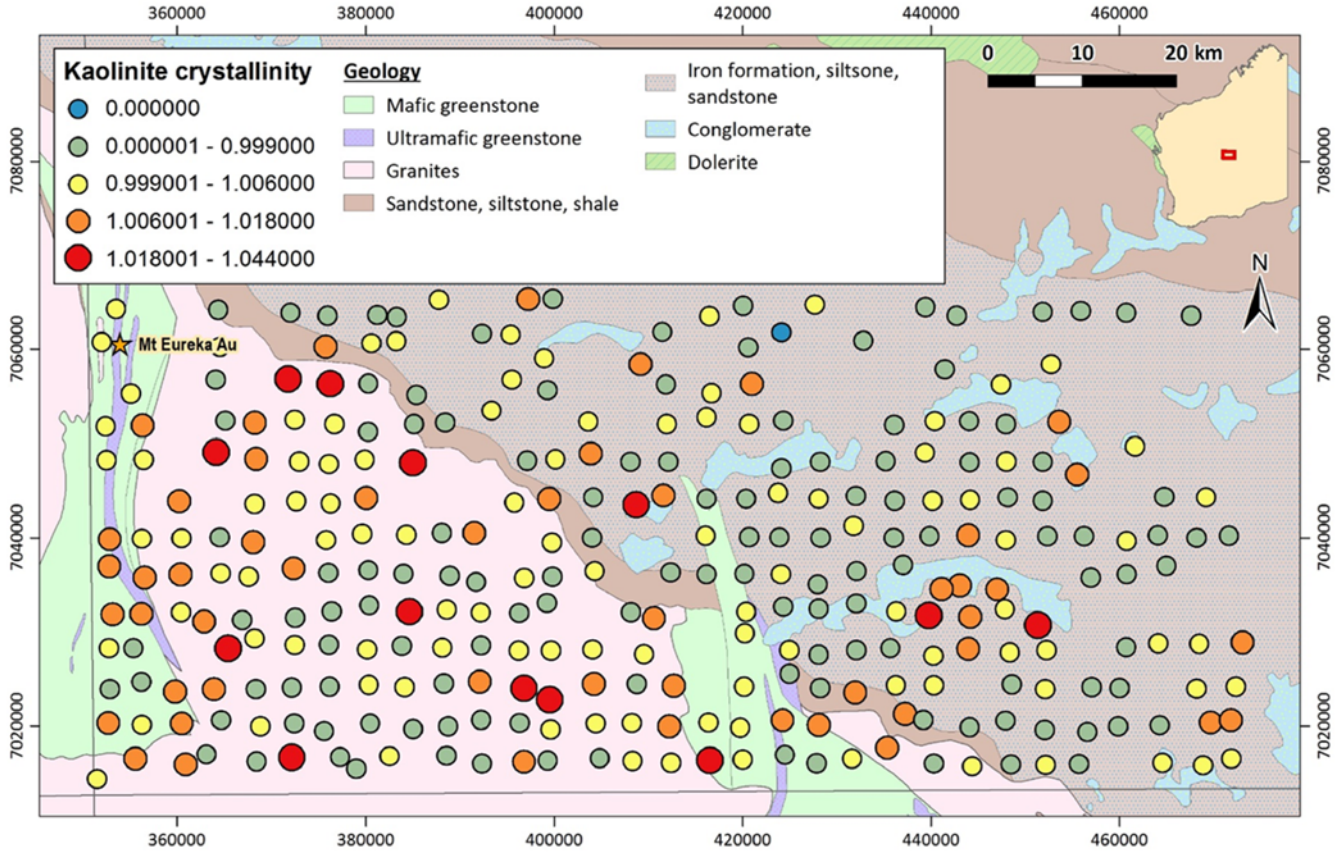

Fig. 23. Kaolinite crystallinity from the 2160 nm feature in the Kingston soils using the ultrafine soils.

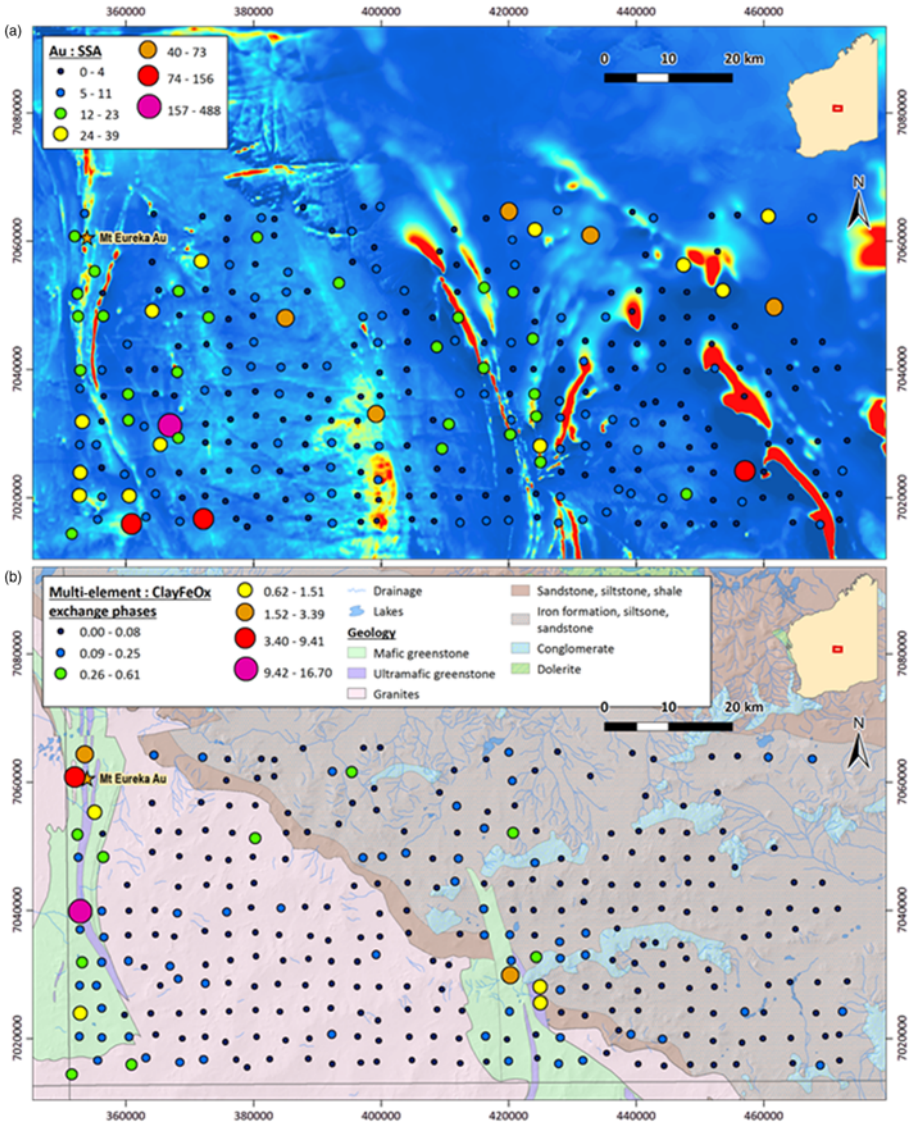

Fig. 24. New potential map products using the UltraFine+™ workflow. (**a**) Gold adjusted for the specific surface area (SSA) of the samples overlying the magnetics. (**b**) A typical multi-element index that is now adjusted with respect to an increase in exchange phases with clay and Fe oxides. Geology is generalized and based on the data from GSWA (2014).

Conclusions

The new adaption of methods known as UltraFine+™ extracts the <2 µm fraction of soils and sediments, provides an assay of the geochemistry, and combines this with additional spectral mineralogy proxies and physicochemical properties to improve soil analysis for Au and base-metal exploration. Applying this to exploration examples showed promising results at a number of small orientation test sites. Of most relevance, the study revealed a marked decrease in censored results for Au (from *c.* 70% to 10% below detection limit) using historical samples and re-assaying them to produce a new geochemistry map of the Kingston 1:250 000 map sheet. The new maps show geochemistry and some example indices for mineral exploration and lithology mapping, as well as example map products of new interpretations using the additional spectral mineralogy proxies or particle-size variation. Adding spectral mineralogy, particle size and other physicochemical parameters to this style of mapping is valuable, is not commonly done, and is certainly not integrated with the interpretation of the geochemical data. Future research will improve the UltraFine+™ method, particularly building algorithms to cloud-process the various data streams, and this should be part of the service from commercial laboratories in the future. The application of the <2 µm particle-size separation and the UltraFine+™ workflow importantly demonstrate the additional value from (re-)assaying regional soil and sediment samples to generate new targets and improve regional geochemical maps. This exercise can be applied to new greenfields surveys, and when exploration budgets are lean, applied to abundant, historically collected samples.

Acknowledgements We acknowledge the analytical support from LabWest and the M462 Ultrafine Project sponsors MRIWA, GSWA, AngloGold Ashanti, Antipa Minerals, Encounter Resources, First Quantum Minerals, Gold Road Resources, Northern Star Resources and Southern Gold. We also thank the CSIRO internal reviewers (Walid Salama and Robert Thorne), and the GEEA external reviewers (Dennis Arne, Bruno Lemiere and anonymous) who improved this publication.

Author contributions RRPN: Conceptualization (Lead), Formal Analysis (Lead), Funding Acquisition (Lead), Methodology (Lead), Writing – Original Draft (Lead); PAM: Conceptualization (Supporting), Funding Acquisition (Supporting), Investigation (Supporting), Writing – Review & Editing (Supporting); RRA: Funding Acquisition (Supporting), Investigation (Supporting), Project Administration (Supporting), Supervision (Supporting), Writing – Review & Editing (Equal); ICL: Data Curation (Supporting), Formal Analysis (Supporting), Investigation (Supporting), Methodology (Supporting), Writing – Original Draft (Supporting); GTP: Data Curation (Equal), Formal Analysis (Supporting), Investigation (Supporting), Methodology (Supporting).

Funding Financial support was provided by the Minerals and Energy Research Institute of Western Australia (grant to RRPN), the Geological Survey of Western Australia (grant to RRPN), and CSIRO Mineral Resources.

Scientific editing by Scott Wood

References

Adamides, N.G. 1998. *Geology of the Doolgunna 1:100 000 Sheet*. Western Australia Geological Survey, 1:100 000 Geological Series. Explanatory Notes. Department of Minerals and Energy, Perth, WA, Australia.

Anand, R.R. & Butt, C.R.M. 2010. A guide for mineral exploration through the regolith in the Yilgarn Craton, Western Australia. *Australian Journal of Earth Sciences*, **57**, 1015–1114, https://doi.org/10.1080/08120099.2010.522823

Anand, R.R. & Paine, M. 2002. Regolith geology of the Yilgarn Craton, Western Australia: Implications for exploration. *Australian Journal of Earth Sciences*, **49**, 3–262, https://doi.org/10.1046/j.1440-0952.2002.00912.x

Anand, R.R., Cornelius, M. & Phang, C. 2007. Use of vegetation and soil in mineral exploration in areas of transported overburden, Yilgarn Craton, Western Australia. *Geochemistry: Exploration, Environment, Analysis*, **7**, 267–288, https://doi.org/10.1144/1467-7873/07-142

Anand, R.R., Lintern, M.J. *et al.* 2009. *AMIRA P778 Final Report Predictive Geochemistry in Areas of Transported Overburden*. CSIRO Exploration and Mining Report P2009/1788.

Anand, R., Lintern, M. *et al.* 2014. Geochemical dispersion through transported cover in regolith-dominated terrains – Towards an understanding of process. *In*: Kelley, K.D. & Golden, H.C. (eds) *Building Exploration Capability for the 21st Century*. Society of Economic Geology Special Publications, **18**, 97–126, https://doi.org/10.5382/SP.18.06

Anand, R.R., Aspandiar, M. & Noble, R.R.P. 2016*a*. A review of metal transfer mechanisms through transported cover with emphasis on the vadose zone within the Australian regolith. *Ore Geology Reviews*, **73**, 394–416, https://doi.org/10.1016/j.oregeorev.2015.06.018

Anand, R.R., Lintern, M.J. *et al.* 2016*b*. The dynamics of gold in regolith change with differing environmental conditions over time. *Geology*, **45**, 127–130, https://doi.org/10.1130/G38591.1

Arne, D. & MacFarlane, B. 2014. Reproducibility of gold analyses in stream sediment samples from the White Gold District and Dawson Range, Yukon Territory, Canada. *Explore*, **164**, 1–10, https://www.appliedgeochemists.org/images/Explore/Explore_Number_164_Sept_2014.pdf

Baker, P.M. 2015. Advances in reconnaissance sampling and geochemical analysis are creating new exploration opportunities in previously sampled terranes. *In*: *Proceedings of the 27th International Applied Geochemistry Symposium 2015*. Association of Applied Geochemists, Ontario, Canada, 11.

Baker, P.M., Agnew, P.A. & Hooper, M. 2015. Using existing, publicly-available data to generate new exploration projects. *In*: *Proceedings of the 27th International Applied Geochemistry Symposium 2015*. Association of Applied Geochemists, Ontario, Canada, 14.

Blewett, R.S., Czarnota, C. & Henson, P.A. 2010. Structural-event framework for the eastern Yilgarn Craton, Western Australia, and its implications for Orogenic gold. *Precambrian Research*, **83**, 203–209, https://doi.org/10.1016/j.precamres.2010.04.004

Bradley, J.J., Sanders, A.J., Varga, Z.S. & Storey, J.M. 1995. *Geochemical Mapping of the Leonora 1:250,000 Sheet*. Western Australia Geological Survey, 1:250 000 Regolith Geochemistry Series Explanatory Notes. Department of Minerals and Energy, Perth, WA, Australia.

Bureau of Meteorology. 2013. Online climate data for Telfer aero station. Australian Government Bureau of Meteorology, http://www.bom.gov.au/ [last accessed August 2013].

Bureau of Meteorology. 2018. Online climate data for Kalgoorlie–Boulder airport station. Australian Government Bureau of Meteorology, http://www.bom.gov.au/ [last accessed September 2018].

Carlson, W.R. 2016. *Heavy minerals in soils from the Athabasca Basin and the implications for exploration geochemistry of uranium deposits at depth*. Master's thesis, Queens University, Kingston, Canada, https://qspace.library.queensu.ca/handle/1974/15203

Chao, T.T. & Zhou, L. 1983. Extraction techniques for selective dissolution of amorphous iron oxides from soils and sediments. *Soil Science Society of America Journal*, **47**, 225–232, https://doi.org/10.2136/sssaj1983.03615995004700020010x

Dominy, S.C., Stephenson, P.R. & Annels, A.E. 2001. Classification and reporting of mineral resources for high-nugget effect gold vein deposits. *Exploration and Mining Geology*, **10**, 215–233, https://doi.org/10.2113/0100215

Encounter Resources. 2016. Encounter secures large scale gold opportunity at Telfer West. ASX release 25 August 2016. Encounter Resources Ltd, West Perth, WA, Australia.

Fang, Q., Hong, H., Zhao, L., Kukolich, S., Ke, Y. & Wang, C. 2018. Visible and near-infrared reflectance spectroscopy for investigating soil mineralogy: A review. *Journal of Spectroscopy*, **2018**, 3168974, https://doi.org/10.1155/2018/3168974

Gee, G.W. & Bauder, J.W. 1986. Particle size analysis. *In*: Klute, A. (ed.) *Methods of Soil Analysis*. American Society of Agronomy, Madison, WI.

Godel, B., González-Álvarez, I., Barnes, S.J., Barnes, S.-J., Parker, P. & Day, P. 2012. Sulfides and sulfarsenides from the Rosie Nickel Prospect, Duketon greenstone belt, Western Australia. *Economic Geology*, **107**, 275–294, https://doi.org/10.2113/econgeo.107.2.275

González-Álvarez, I., Salama, W., Ibrahimi, T. & LeGras, M. 2015. *Geochemical Dispersion of the DeGrussa Deposit within its Associated Palaeodrainage System*. CSIRO Technical Report EP 158718. CSIRO, Kensington, WA, Australia, https://doi.org/10.4225/08/5852dbec874d3

Gray, D.J., Noble, R.R.P., Reid, N., Sutton, G.J. & Pirlo, M.C. 2016. Regional scale hydrogeochemical mapping of the northern Yilgarn Craton, Western Australia: A new technology for exploration in arid Australia. *Geochemistry: Exploration, Environment, Analysis*, **16**, 100–115, https://doi.org/10.1144/geochem2014-333

Grunsky, E.C. 2010. The interpretation of geochemical survey data. *Geochemistry: Exploration, Environment, Analysis*, **10**, 27–74, https://doi.org/10.1144/1467-7873/09-210

GSWA 2014. *1:500 000 State Interpreted Bedrock Geology of Western Australia*. Geological Survey of Western Australia (GSWA), Department of Primary Industry and Resources, Perth, WA, Australia http://geodownloads.dmp.wa.gov.au/Downloads/Metadata_Statements/XML/500K_IBG_WA_2014.xml [last accessed August 2013].

Haest, M., Cudahy, T., Laukamp, C. & Gregory, S. 2012. Quantitative mineralogy from infrared spectroscopic data. I. Validation of mineral abundance and composition scripts at the Rocklea channel iron deposit in Western Australia. *Economic Geology*, **107**, 209–228, https://doi.org/10.2113/econgeo.107.2.209

Hall, G.E.M. 1998. Analytical perspective on trace element species of interest in exploration. *Journal of Geochemical Exploration*, **61**, 1–19, https://doi.org/10.1016/S0375-6742(97)00046-0

Hall, G.E.M., Vaive, J.E., Beer, R. & Hoashi, M. 1996. Selective leaches revisited, with emphasis on the amorphous Fe oxyhydroxide phase extraction. *Journal of Geochemical Exploration*, **56**, 59–78, https://doi.org/10.1016/0375-6742(95)00050-X

Harris, J.F. 1982. Sampling and analytical requirements for effective use of geochemistry in exploration for gold. *In*: Levinson, A.A. (ed.) *Precious Metals in the Northern Cordillera*. Association of Applied Geochemists, Special Volume, **10**, 53–67.

Hawke, M.L., Meffre, S., Stein, H., Hilliard, P., Large, R. & Gemmell, J.B. 2015. Geochronology of the DeGrussa volcanic-hosted massive sulphide deposit and associated mineralisation of the Yerrida, Bryah and Padbury Basins, Western Australia. *Precambrian Research*, **267**, 250–284, https://doi.org/10.1016/j.precamres.2015.06.011

Hawkes, H.E. & Webb, J.S. 1962. *Geochemistry in Mineral Exploration*. Harper and Row, New York.

Kelley, D.L., Hall, G.E.M., Clos, L.G., Hamilton, I.C. & McEwen, R.M. 2003. The use of partial extraction geochemistry for copper exploration in northern Chile. *Geochemistry: Exploration, Environment, Analysis*, **3**, 85–104, https://doi.org/10.1144/1467-787302-048

Kendrick, P. 2001. Little Sandy Desert (LSD1 - Rudall subregion in A Biodiversity Audit of Western Australia's 53 Biogeographical subregions. Department of Conservation and Land Management Canning Resources Pty Ltd.

Kojan, C.J., Faulkner, J.A. & Sanders, A.J. 1996. *Geochemical Mapping of the Sir Samuel 1:250 000 Sheet*. Western Australia Geological Survey, 1:250 000 Regolith Geochemistry Series Explanatory Notes. Department of Minerals and Energy, Perth, WA, Australia.

Lampinen, H.M., Laukamp, C., Occhipinti, S.A. & Hardy, L. 2019. Mineral footprints of the Paleoproterozoic sediment-hosted Abra Pb–Zn–Cu–Au deposit Capricorn Orogen, Western Australia. *Ore Geology Reviews*, **104**, 436–461, https://doi.org/10.1016/j.oregeorev.2018.11.004

Laukamp, C., Salama, W. & Gonzalez-Alvarez, I. 2015. Proximal and remote spectroscopic characterisation of regolith in the Albany–Fraser Orogen (Western Australia). *Ore Geology Reviews*, **73**, 540–554, https://doi.org/10.1016/j.oregeorev.2015.10.003

LeGras, M., Laukamp, C., Lau, I. & Mason, P. 2018. *NVCL Spectral Reference Library – Phyllosilicates Part 2: Micas*. CSIRO Technical Report EP 183095. CSIRO, Kensington, WA, Australia.

Leybourne, M.I. & Rice, S. 2013. Determination of gold in soils and sediments by fire assay or aqua regia digestion: Choosing the optimal method. *Explore*, **158**, 1–10, https://www.appliedgeochemists.org/images/Explore/Explore_Number_158_March_2013.pdf

Li, M., Xi, X., Xiao, G., Cheng, H., Yang, Z., Zhou, G., Ye, J. & Li, Z. 2014. National multi-purpose regional geochemical survey in China. *Journal of Geochemical Exploration*, **139**, 21–30, https://doi.org/10.1016/j.gexplo.2013.06.002

MacKenzie, D., Craw, D. & Finnigan, C. 2015. Lithologically controlled invisible gold, Yukon, Canada. *Mineralium Deposita*, **50**, 141–157, https://doi.org/10.1007/s00126-014-0532-5

Malvern Instruments. 2011. Chapter 5: Viewing measurement results. *In*: *Mastersizer 3000 User Manual*. Malvern Instruments, Malvern, Worcestershire, UK.

McClenaghan, M.B. & Paulen, R.C. 2018. Application of till mineralogy and geochemistry to mineral exploration. *In*: Menzies, J. & van der Meer, J.J.M. (eds) *Past Glacial Environments*. 2nd edn. Elsevier, Amsterdam, 689–751.

McCuaig, T.C., Beresford, S. & Hronsky, J. 2010. Translating the mineral systems approach into an effective exploration targeting system. *Ore Geology Reviews*, **38**, 128–138, https://doi.org/10.1016/j.oregeorev.2010.05.008

Morris, P.A. 2013. Fine fraction regolith chemistry from the East Wongatha area, Western Australia: tracing bedrock and mineralization through thick cover. *Geochemistry: Exploration, Environment, Analysis*, **13**, 21–40, https://doi.org/10.1144/geochem2012-141

Morris, P.A. & Sanders, A.J. 2001. The effect of sample medium on regolith chemistry over greenstone belts in the northern Eastern Goldfields of Western Australia. *Geochemistry: Exploration, Environment, Analysis*, **1**, 201–210, https://doi.org/10.1144/geochem.1.3.201

Morris, P.A. & Verren, A.L. 2001. *Geochemical Mapping of the Byro 1:250 000 Sheet*. Western Australia Geological Survey, 1:250 000 Regolith Geochemistry Series Explanatory Notes. Department of Minerals and Energy, Perth, WA, Australia.

Myers, J.S. 1997. Preface: Archaean geology of the Eastern Goldfields of Western Australia – regional overview. *Precambrian Research*, **83**, 1–10, https://doi.org/10.1016/S0301-9268(97)00002-8

Myers, J.S. & Hocking, R.M. (compilers). 1998. *Simplified Geological Map of Western Australia 1:2 500 000*. 13th edn. Western Australia Geological Survey, Perth, WA, Australia.

Nichol, I., Closs, L.G. & Lavin, O.P. 1989. Sample representativity with reference to gold exploration. *In*: Garland, G.D. (ed.) *Proceedings of Exploration '87*. Association of Applied Geochemists, Special Volume, **3**, 609–624.

Noble, R.R.P. 2012. Transported cover in northwestern Victoria, Australia – An impediment to geochemical exploration for gold. *Journal of Geochemical Exploration*, **112**, 139–151, https://doi.org/10.1016/j.gexplo.2011.08.006

Noble, R.R,P., Cavaliere, M., Morris, P., Pinchand, T. & Hough, R. 2013. Determination of micro and nanoparticulate fraction gold in regolith. *Explore*, **159**, 1–13, https://www.appliedgeochemists.org/images/Explore/Explore%20Number%20159%20June%202013.pdf

Noble, R.R.P., Anand, R.R., Gray, D.J. & Cleverley, J.S. 2017. Metal migration at the DeGrussa Cu–Au sulphide deposit, Western Australia: Soil, vegetation and groundwater studies. *Geochemistry: Exploration, Environment, Analysis*, **17**, 124–142, https://doi.org/10.1144/geochem2016-416

Noble, R.R.P., Seneshen, D.M., Lintern, M.J., Anand, R.R., Pagès, A. & Pinchand, G.T. 2018. Soil-gas and weak partial soil extractions for nickel exploration through transported cover in Western Australia. *Geochemistry: Exploration, Environment, Analysis*, **18**, 31–45, https://doi.org/10.1144/geochem2017-026

Noble, R.R.P., Lau, I.C., Anand, R.R. & Pinchand, G.T. 2019. Refining fine fraction soil extraction methods and analysis for mineral exploration. *Geochemistry: Exploration, Environment, Analysis*, https://doi.org/10.1144/geochem2019-008

Pye, K.J., Morris, P.A. & McGuiness, S.A. 2000. *Geochemical Mapping of the Kingston 1:250 000 Sheet*. Western Australia Geological Survey, 1:250 000 Regolith Geochemistry Series Explanatory Notes. Department of Minerals and Energy, Perth, WA, Australia.

Reeves, J.B. & Smith, D.B. 2009. The potential of mid- and near-infrared diffuse reflectance spectroscopy for determining major- and trace-element concentrations in soils from a geochemical survey of North America. *Applied Geochemistry*, **24**, 1472–1481, https://doi.org/10.1016/j.apgeochem.2009.04.017

Reimann, C. & de Caritat, P. 2012. New soil composition data for Europe and Australia: Demonstrating comparability, identifying continental-scale processes and learning lessons for global geochemical mapping. *Science of the Total Environment*, **416**, 239–252, https://doi.org/10.1016/j.scitotenv.2011.11.019

Reimann, C., Filzmoser, P., Garrett, R.G. & Dutter, R. 2010. *Statistical Data Analysis Explained*. John Wiley and Sons, Chichester, UK.

Robertson, I.D.M. 1999. Origins and applications of size fractions of soils overlying the Beasley Creek gold deposit, Western Australia. *Journal of Geochemical Exploration*, **66**, 99–113, https://doi.org/10.1016/S0375-6742(99)00012-6

Sader, J., Benn, C., Zhivkov, N., Jeleva, T. & Anderson, R. 2018. Soil clay fraction geochemistry for surficial exploration: a case study from the Tethyan Belt. *In*: RFG 2018 – Resources for Future Generations Conference Proceedings, Vancouver, Canada. Society of Economic Geologists, Littleton, CO, Abstract 2469.

Salama, W., Anand, R.R. & Kidder J., Pinchand, T., 2016. Multi-scale detection of buried mineralization and lithology through Kalahari transported cover in NW Botswana. Paper 566 (Abstract) presented at the 35th International Geological Congress, 27 August–4 September 2018, Cape Town, South Africa, https://www.americangeosciences.org/igc/13602

Salminen, R. 2011. Geochemical mapping; past, present, future. *In*: *25th International Applied Geochemistry Symposium Programme and Abstracts, 22–26 August 2011, Rovaniemi, Finland*. Finnish Association of Mining and Metallurgical Engineers, Helsinki, 51–52.

Sanders, A.J., Morris, P.A., Subramanya, A.G. & Faulkner, J.A. 1997. *Geochemical Mapping of the Mount Phillips 1:250 000 Sheet*. Western Australia Geological Survey, 1:250 000 Regolith Geochemistry Series Explanatory Notes. Department of Minerals and Energy, Perth, WA, Australia.

Scott, K.M., Yang, K. & Huntington, J.F. 1998. *The Application of Spectral Reflectance Studies of Chlorites in Exploration*. CSIRO Exploration and Mining Report 439R. CSIRO, Sydney, Australia.

Smith, D.B., Woodruff, L.G., O'Leary, R.M., Cannon, W.F., Garrett, R.G., Kilburn, J.E. & Goldhaber, M.B. 2009. Pilot studies for the North American Soil Geochemical Landscapes Project – Site selection, sampling protocols, analytical methods, and quality control protocols. *Applied Geochemistry*, **24**, 1357–1368, https://doi.org/10.1016/j.apgeochem.2009.04.008

Stanley, C.R. 2006. On the special application of Thompson–Howarth error analysis to geochemical variables exhibiting a nugget effect. *Geochemistry: Exploration, Environment, Analysis*, **6**, 357–368, https://doi.org/10.1144/1467-7873/06-111

Stanley, C.R. & Lawie, D. 2007. Average relative error in geochemical determinations: classification, calculation, and a plea for consistency. *Exploration and Mining Geology*, **16**, 267–275, https://doi.org/10.2113/gsemg.16.3-4.267

Toft, P.B., Arkani-Hamed, J. & Haggerty, S.E. 1990. The effects of serpentinization on density and magnetic susceptibility: a petrophysical model. *Physics of the Earth and Planetary Interiors*, **65**, 137–157, https://doi.org/10.1016/0031-9201(90)90082-9

van Geffen, P.W.G., Kyser, K.T., Oates, C.J. & Ihlenfeld, C. 2012. Till and vegetation geochemistry at the Talbot VMS Cu–Zn prospect, Manitoba, Canada: implications for mineral exploration. *Geochemistry: Exploration, Environment, Analysis*, **12**, 67–88, https://doi.org/10.1144/1467-7873/11-RA-066

van Geffen, P.W.G., Kyser, K.T., Oates, C.J. & Ihlenfeld, C. 2015. Evaluation of partial digestions for soils to detect a deeply buried VMS Cu–Zn prospect in boreal forests. *Geochemistry: Exploration, Environment, Analysis*, **15**, 27–38, https://doi.org/10.1144/geochem2011-065

Wainwright, A.J., Simmons, A.T., Finnigan, C.S., Smith, T.R. & Carpenter, R.L. 2011. Geology of new gold discoveries in the Coffee Creek area, White Gold District, west-central Yukon. *In*: MacFarlane, K.E., Weston, L.H. & Relf, C. (eds) *Yukon Exploration and Geology 2010*. Yukon Geological Survey, Whitehorse, Yukon, Canada, 233–247.

Wang, X., Xie, X. & Ye, S. 1995. Concepts for geochemical gold exploration based on the abundance and distribution of ultrafine gold. *Journal of Geochemical Exploraiton*, **55**, 93–101, https://doi.org/10.1016/0375-6742(95)00026-7

Wang, X., Wen, X. *et al.* 2007. Vertical variations and dispersion of elements in arid desert regolith: A case study from the Jinwozi gold deposit, northwestern China. *Geochemistry: Exploration, Environment, Analysis*, **7**, 163–171, https://doi.org/10.1144/1467-7873/07-131

Williams, I.R. 1975. Eastern Goldfields province. *In*: *Geology of Western Australia*. Geological Survey of Western Australia Memoirs, **2**, 33–55, http://dmpbookshop.eruditetechnologies.com.au/product/the-geology-of-western-australia.do

Winterburn, P.A., Noble R.R.P. & Lawie, D., 2019. Advances in exploration geochemistry, 2007–2017 and beyond. *Geochemistry: Exploration, Environment, Analysis*, **19**, https://doi.org/10.1144/geochem2019-030